Supporting information

Random Structural Modification of a Low Band Gap BODIPY-Based Polymer

Léo Bucher,[a,b] Shawkat M. Aly,[a] Nicolas Desbois,[b] Paul-Ludovic Karsenti,[a] Claude P. Gros,[b]* and Pierre D. Harvey[a]*

[a] Département de Chimie, Université de Sherbrooke, 2500, Bd de l'Université J1K 2R1 Sherbrooke, QC, Canada. Email: Pierre.Harvey@USherbrooke.ca

[b] Université de Bourgogne Franche-Comté, ICMUB (UMR CNRS 6302), 9, Avenue Alain Savary, BP 47870, 21078 Dijon Cedex, France. Email: Claude.Gros@u-bourgogne.fr

FIGURES

Characterization of **M1**

Characterization of **M2**

Characterization of **1**

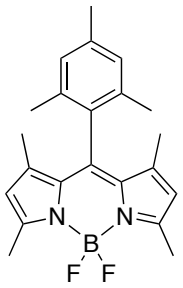

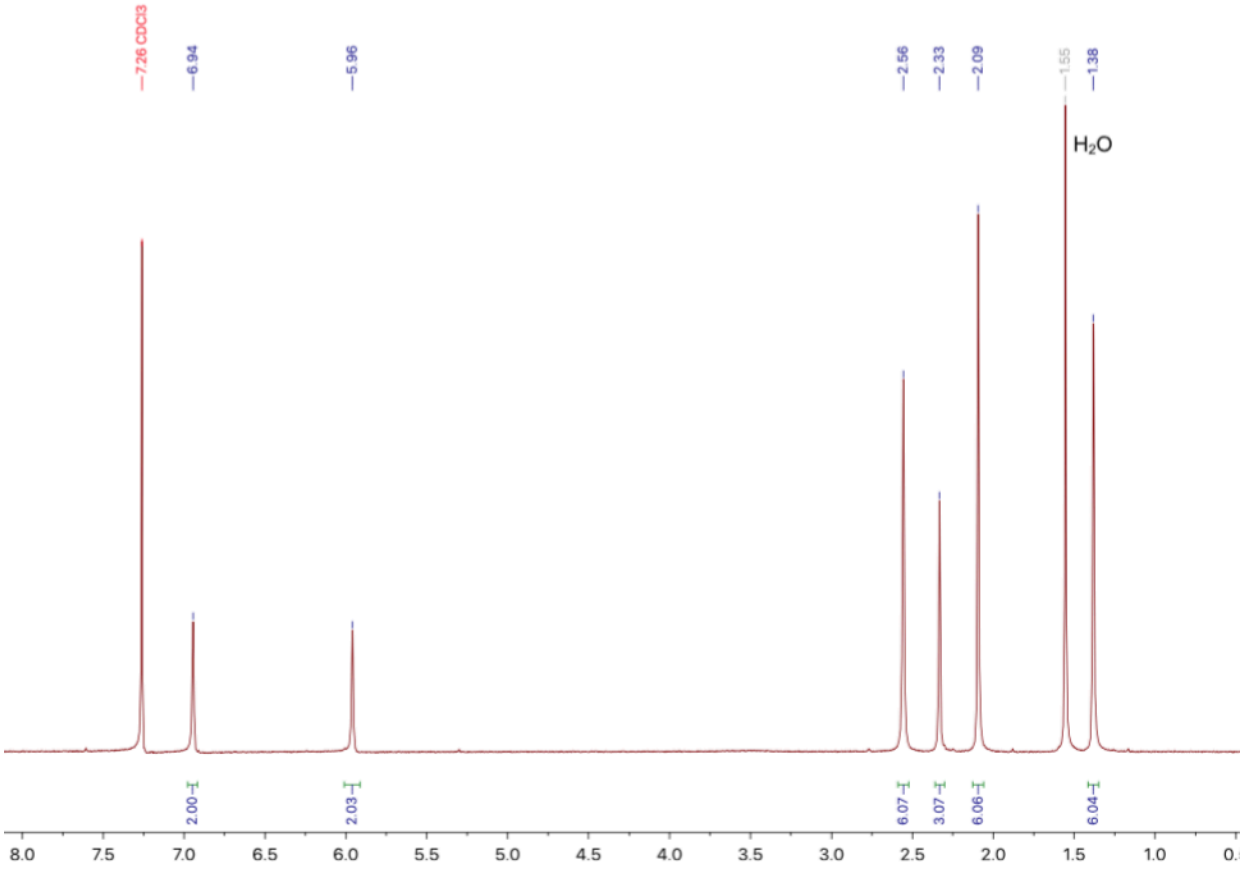

Figure S1: ^{1}H NMR spectrum of **1** (300 MHz, $CDCl_3$, δ ppm)

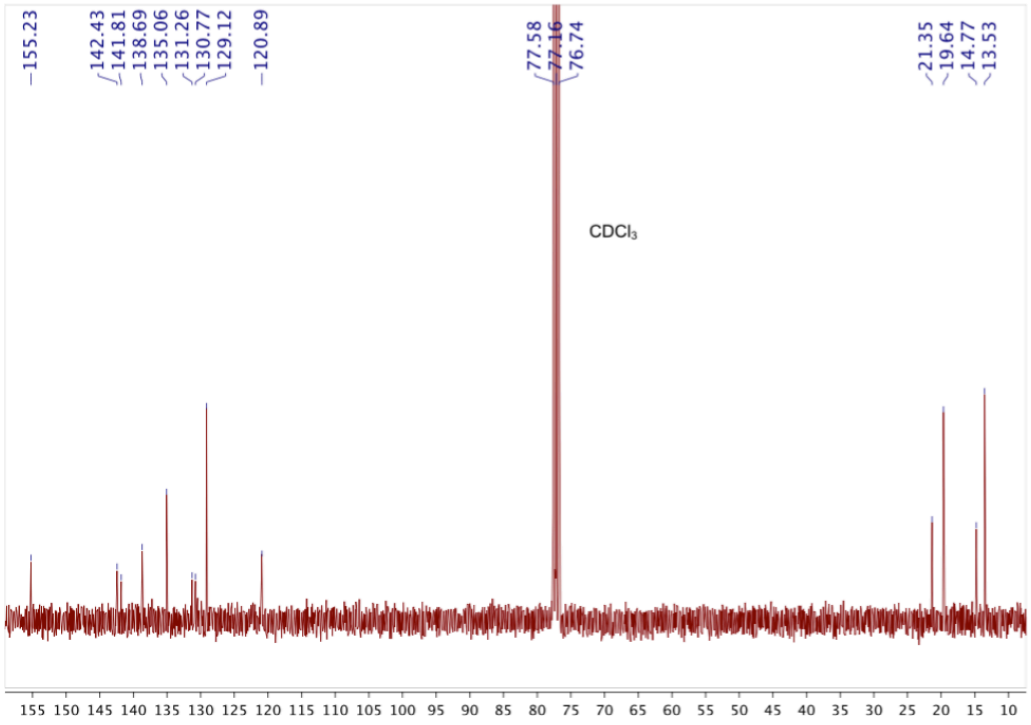

Figure S2: ^{13}C NMR spectrum of **1** (75 MHz, $CDCl_3$, δ ppm)

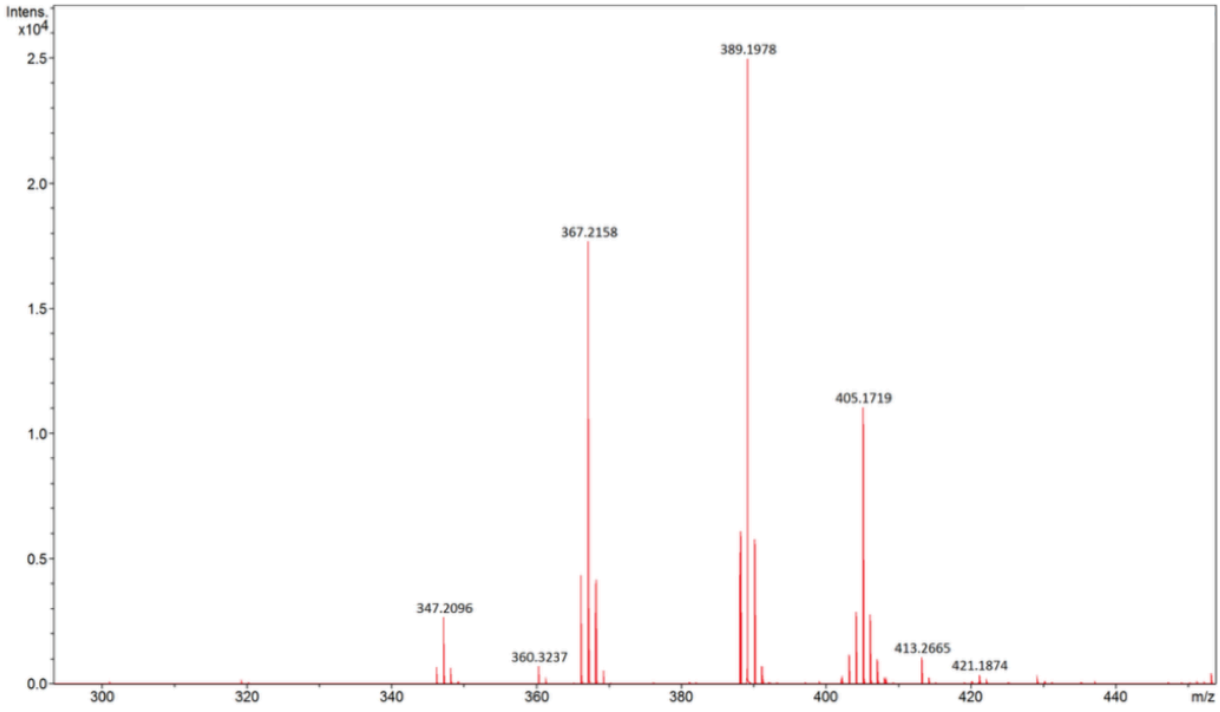

Figure S3: ESI-MS spectrum of **1**

Characterization of **2**

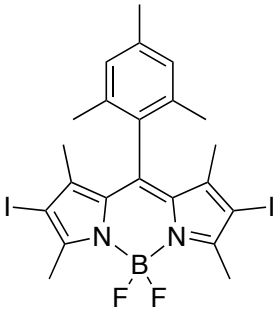

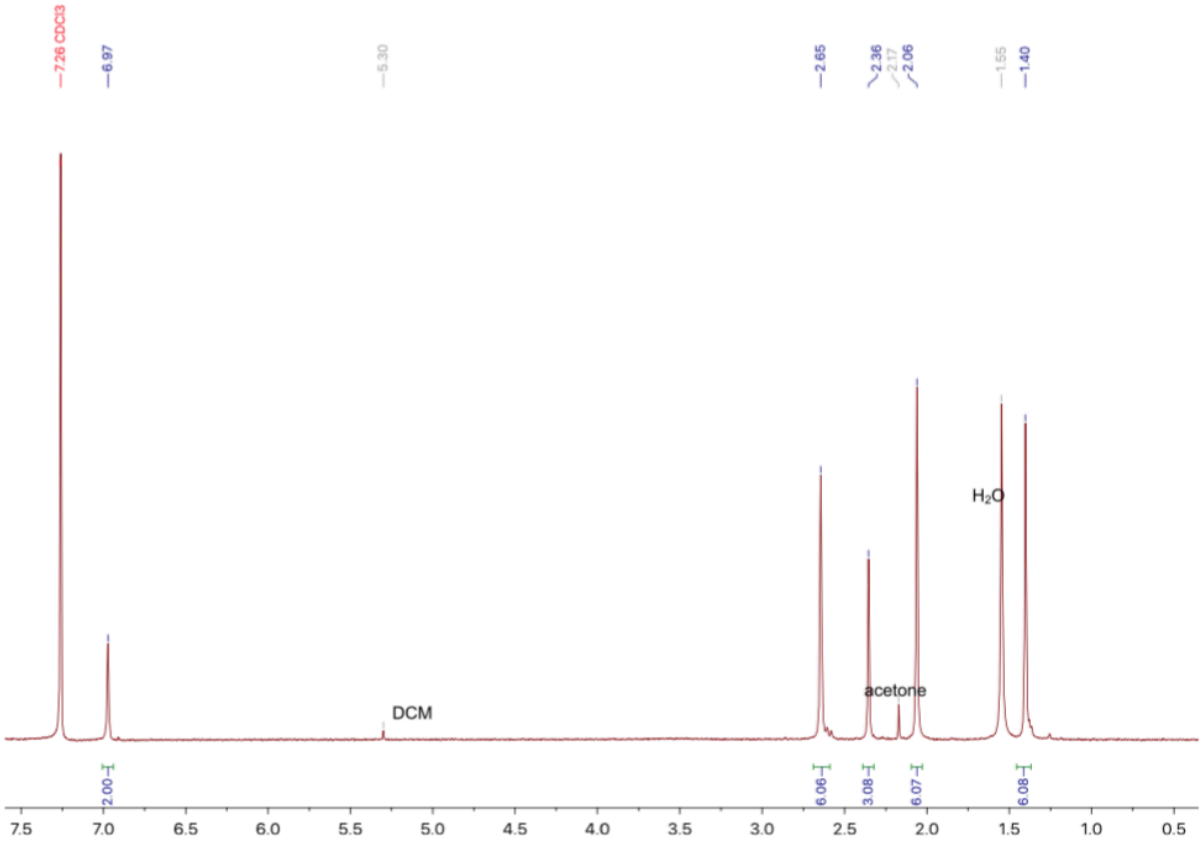

Figure S4: ^{1}H NMR spectrum of **2** (300 MHz, $CDCl_3$, δ ppm)

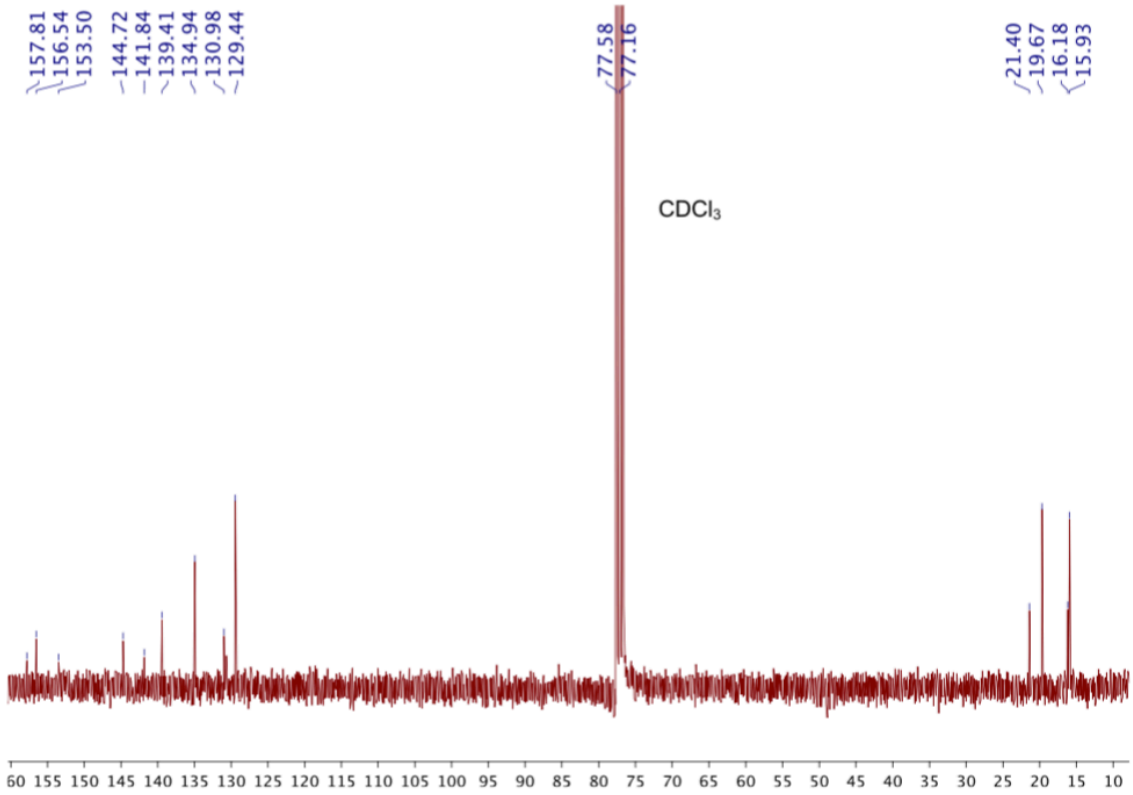

Figure S5: ^{13}C NMR spectrum of **2** (75 MHz, $CDCl_3$, δ ppm)

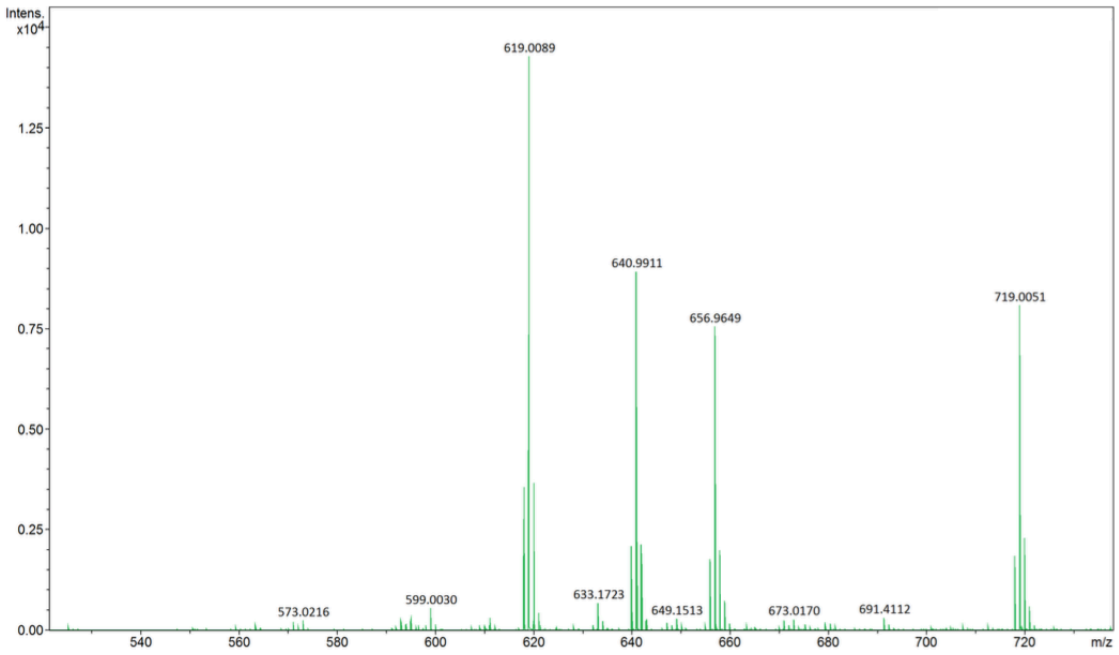

Figure S6: ESI-MS spectrum of **2**

Characterization of **3**

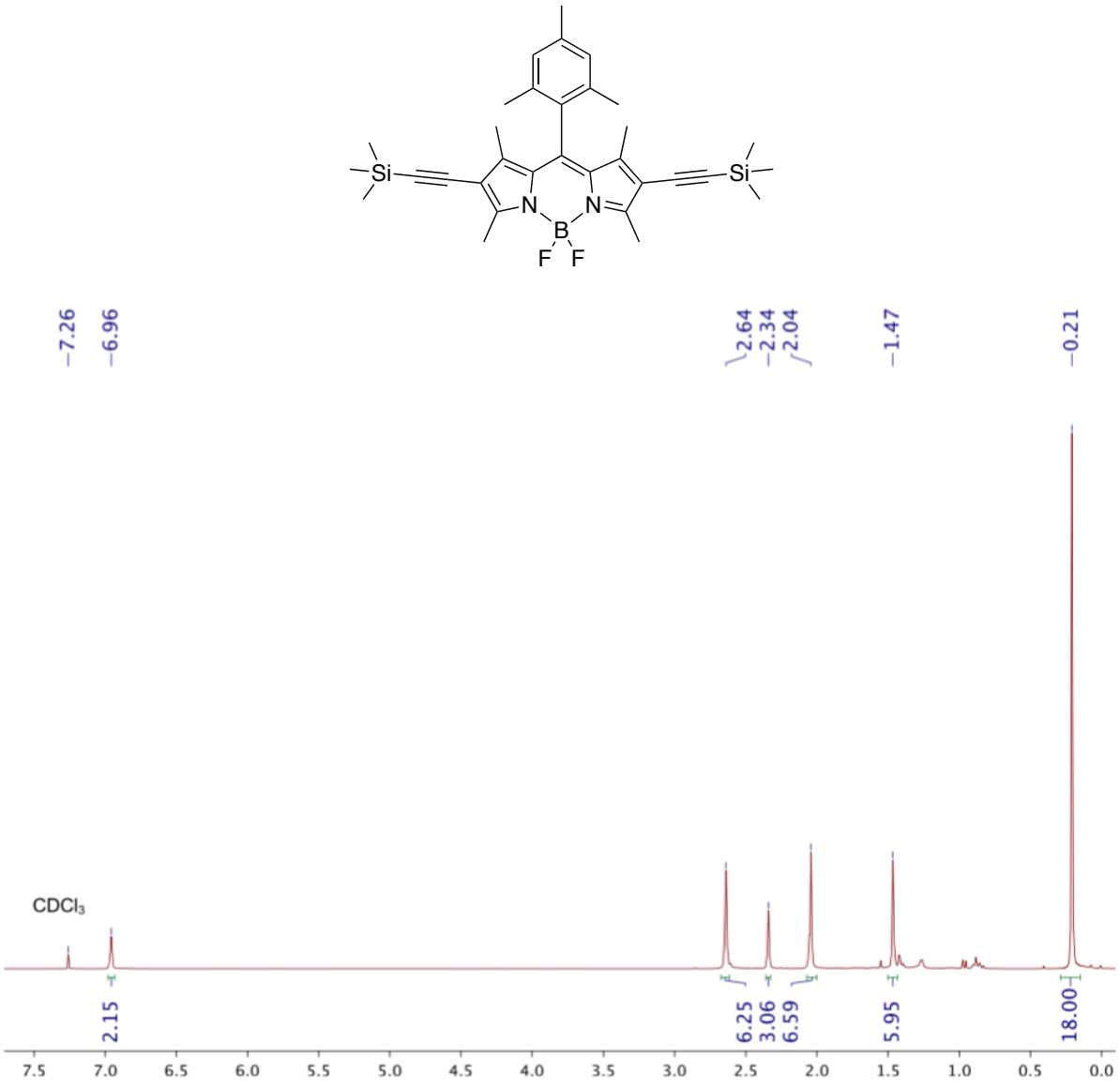

Figure S7: ^{1}H NMR spectrum of **3** (300 MHz, $CDCl_3$, δ ppm)

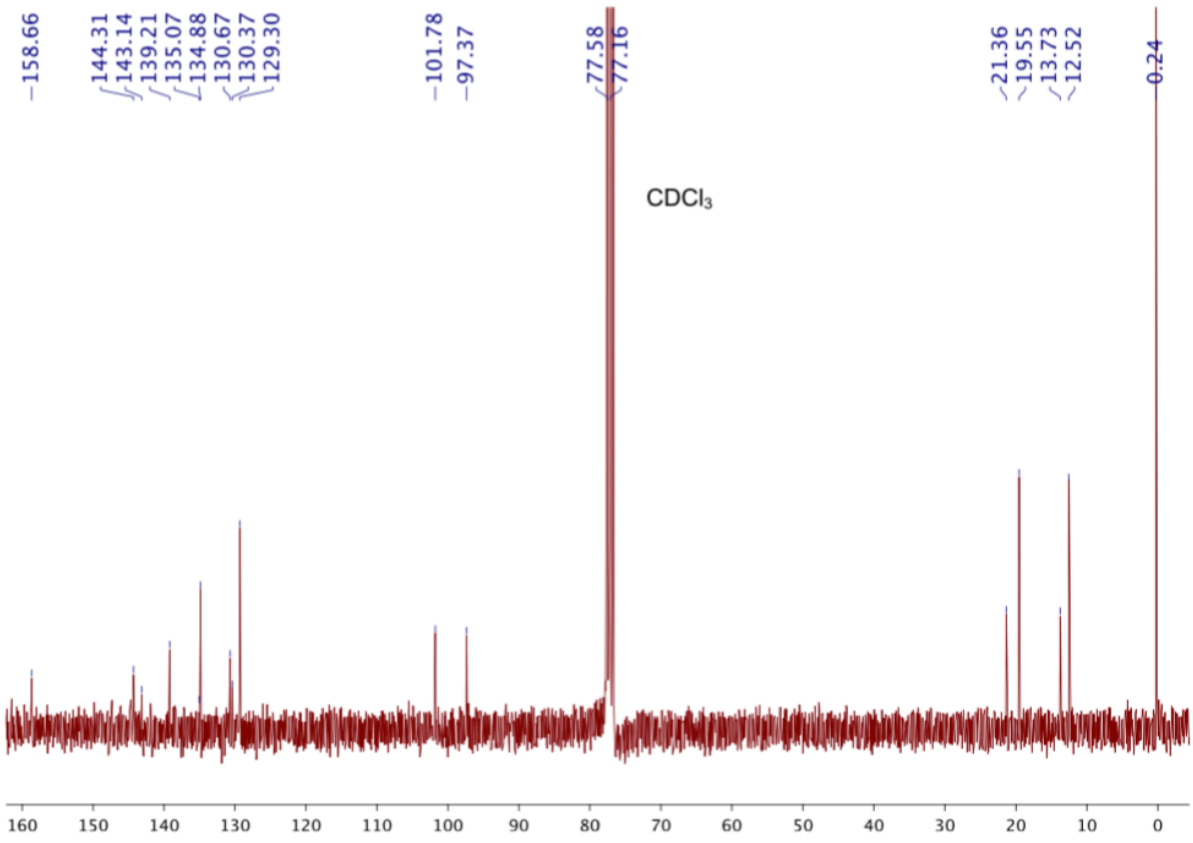

Figure S8: ^{13}C NMR spectrum of **3** (75 MHz, $CDCl_3$, δ ppm)

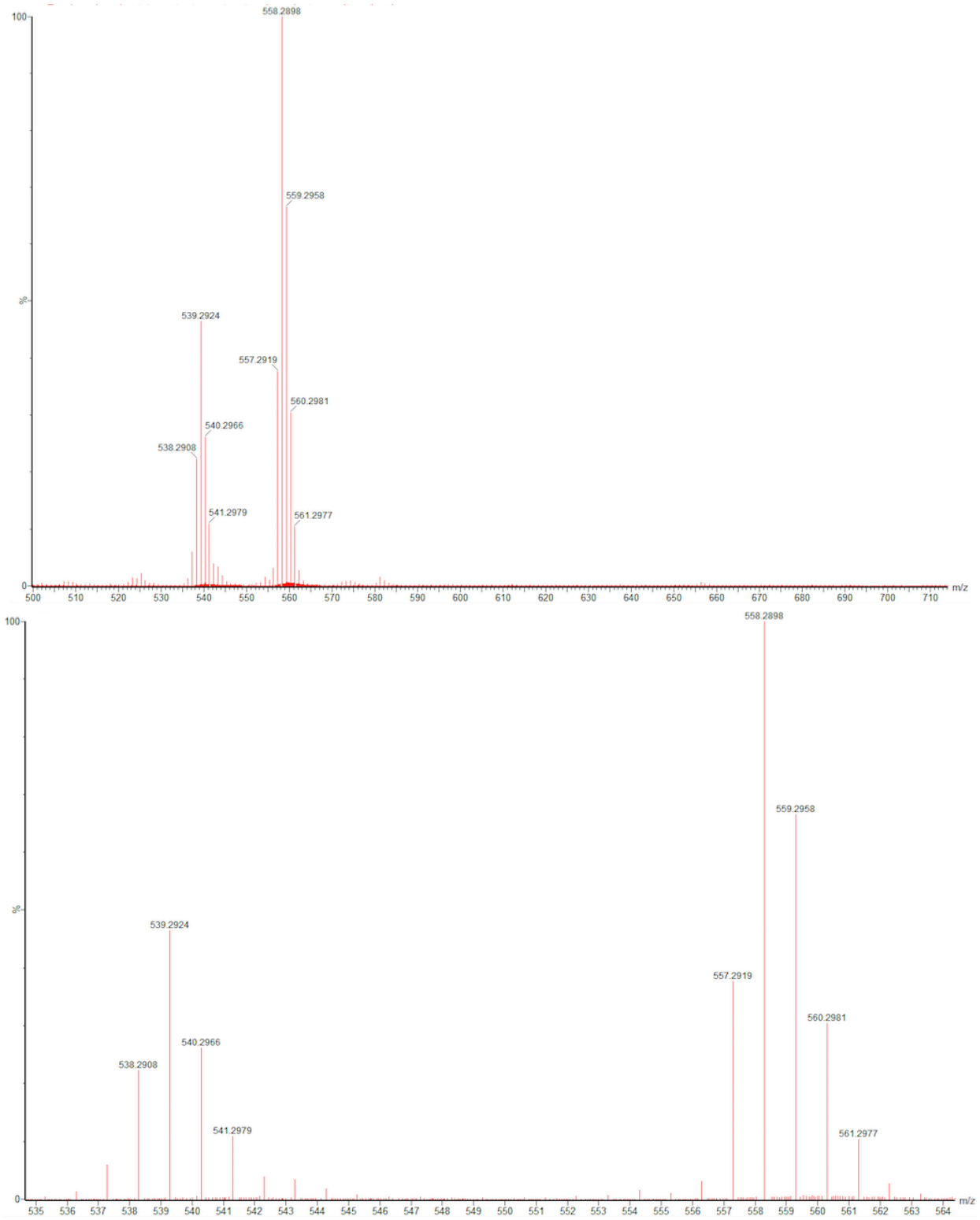

Figure S9: MALDI/TOF-MS full (top) and zoom (bottom) spectra of **3**

Characterization of **4**

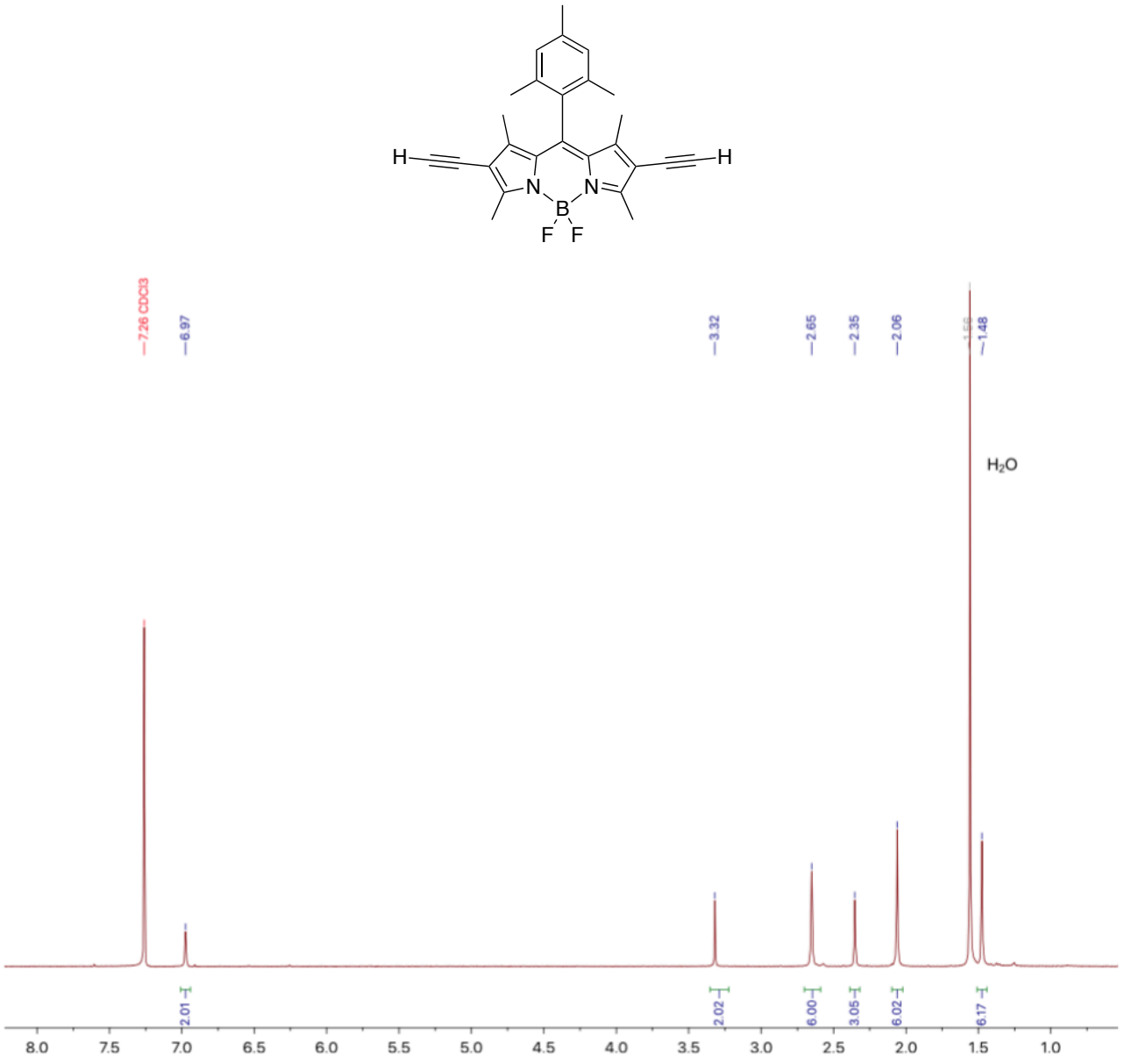

Figure S10: ^{1}H NMR spectrum of **4** (300 MHz, $CDCl_3$, δ ppm)

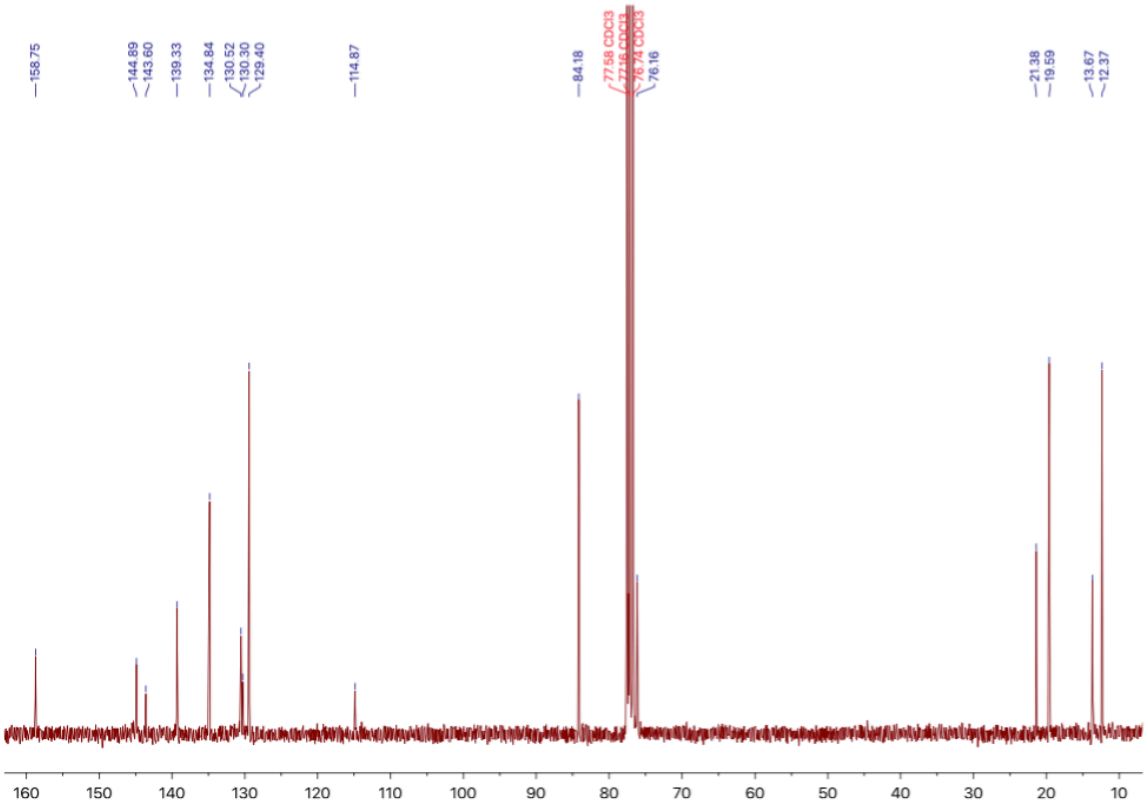

Figure S11: ^{13}C NMR spectrum of **4** (75 MHz, $CDCl_3$, δ ppm)

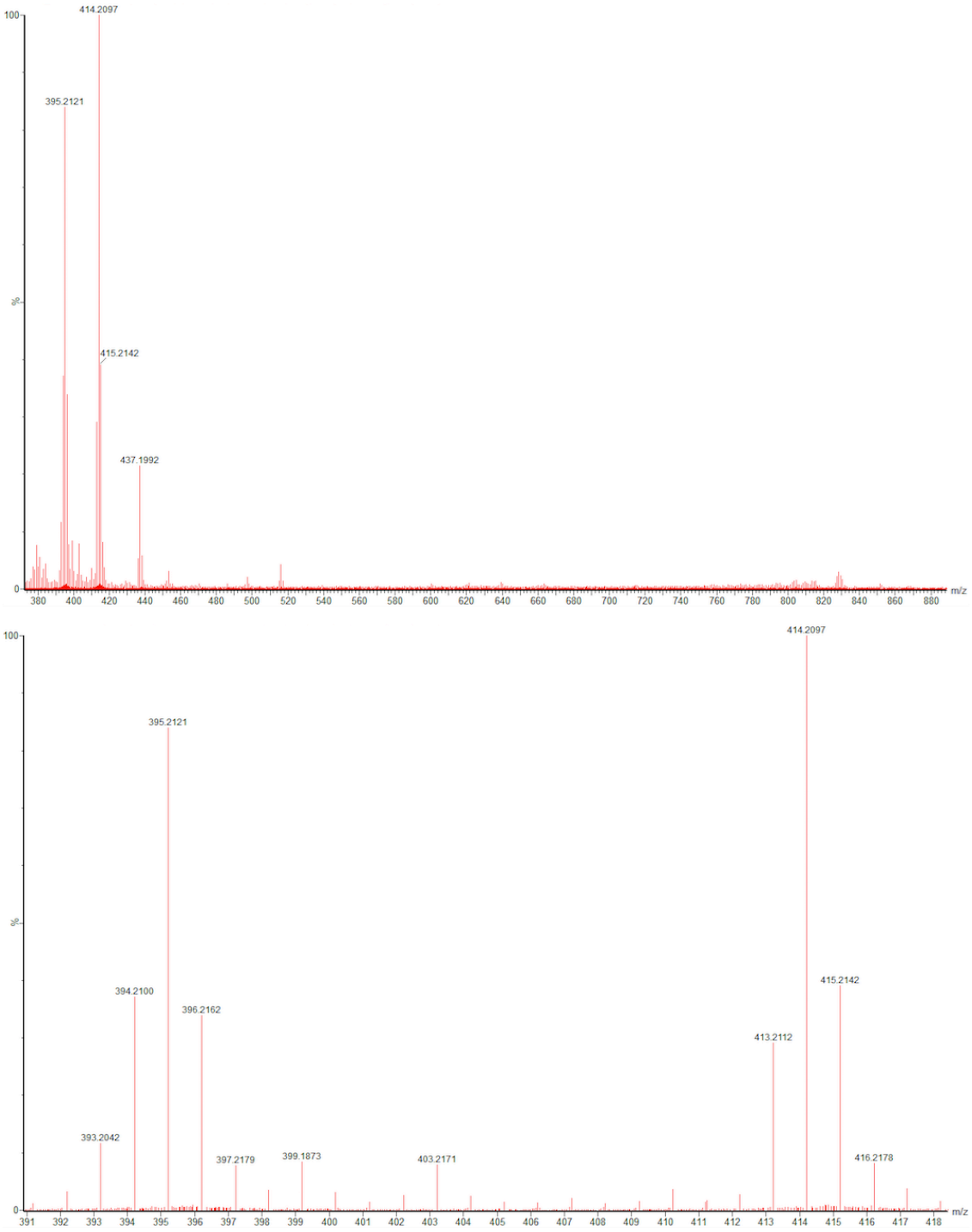

Figure S12: MALDI/TOF-MS full (top) and zoom (bottom) spectra of **4**

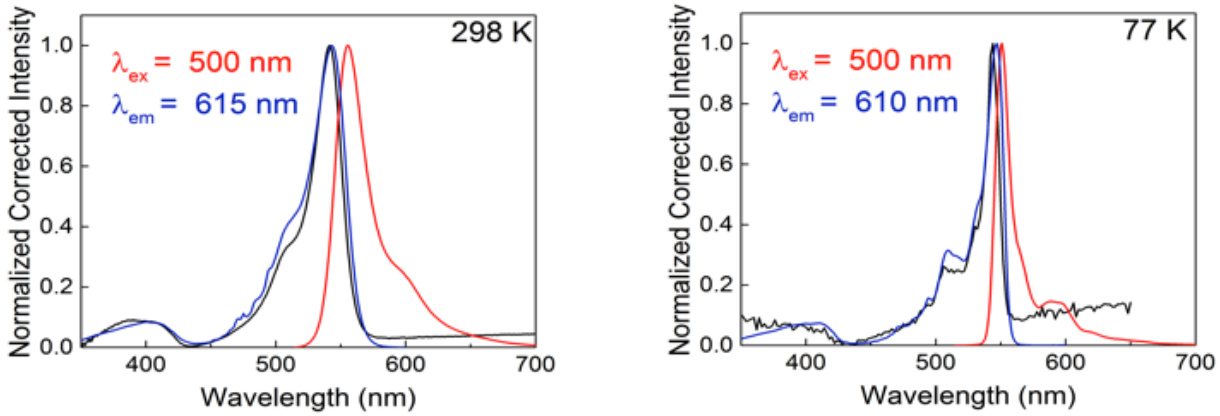

Figure S13: Absorption (black), emission (red), excitation (blue) of **4** at 298 K and 77 K in 2-MeTHF

Characterization of **5**

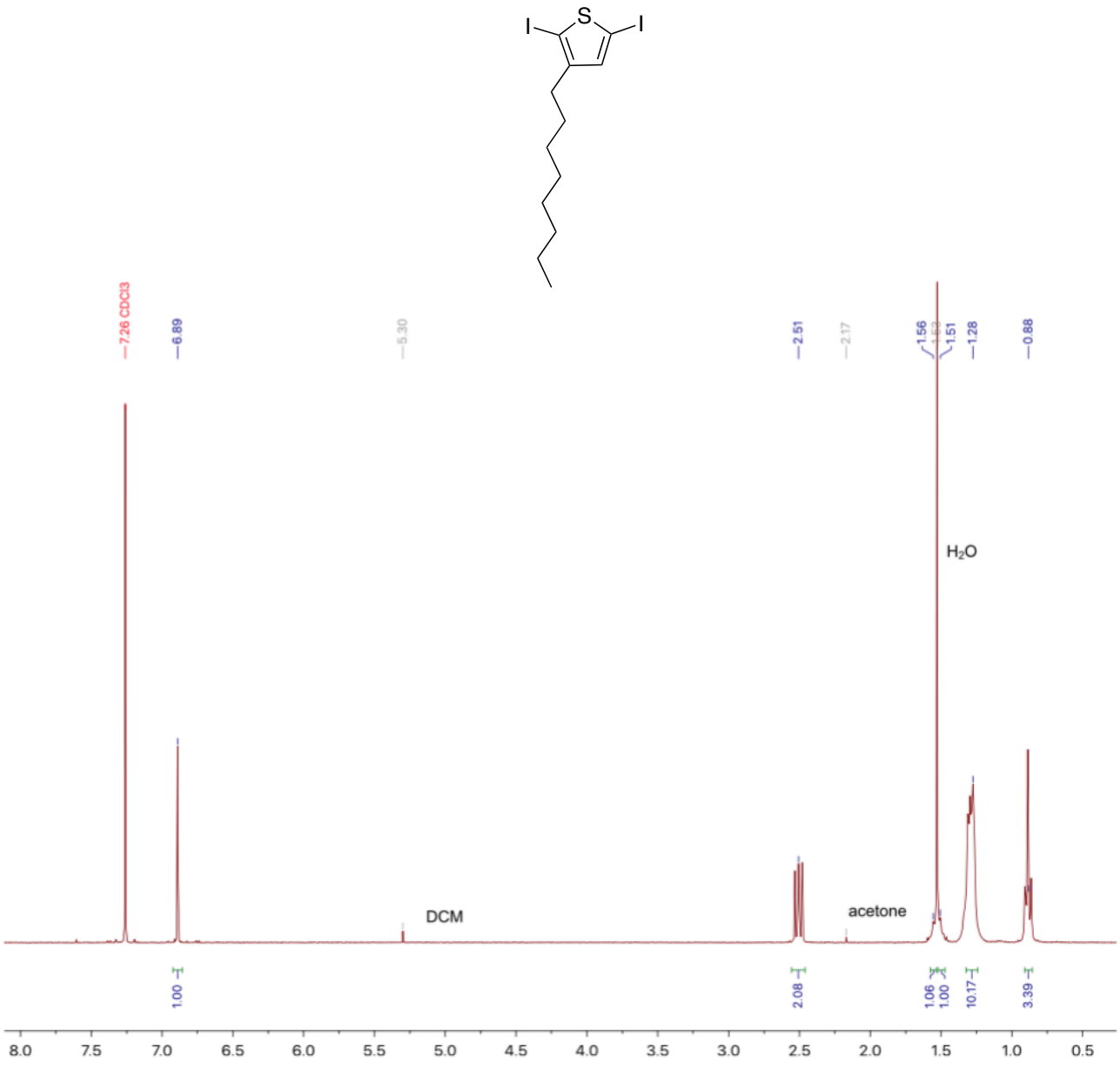

Figure S14: ^{1}H NMR spectrum of **5** (300 MHz, $CDCl_3$, δ ppm)

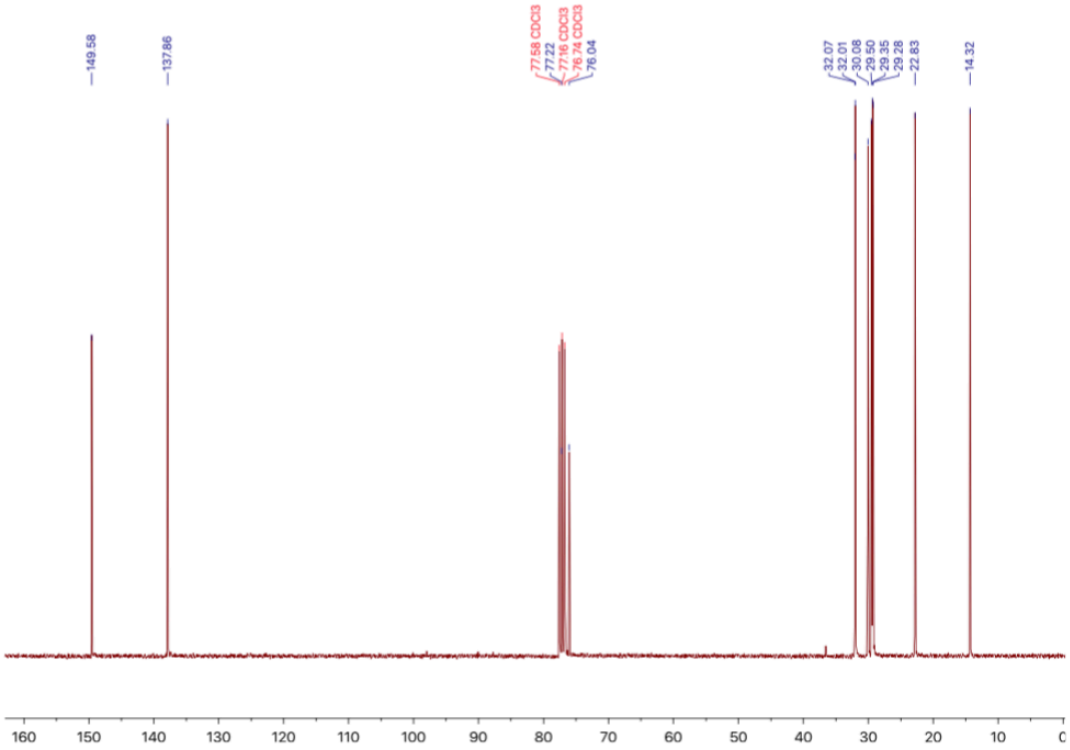

Figure S15: ^{13}C NMR spectrum of **5** (75 MHz, $CDCl_3$, δ ppm)

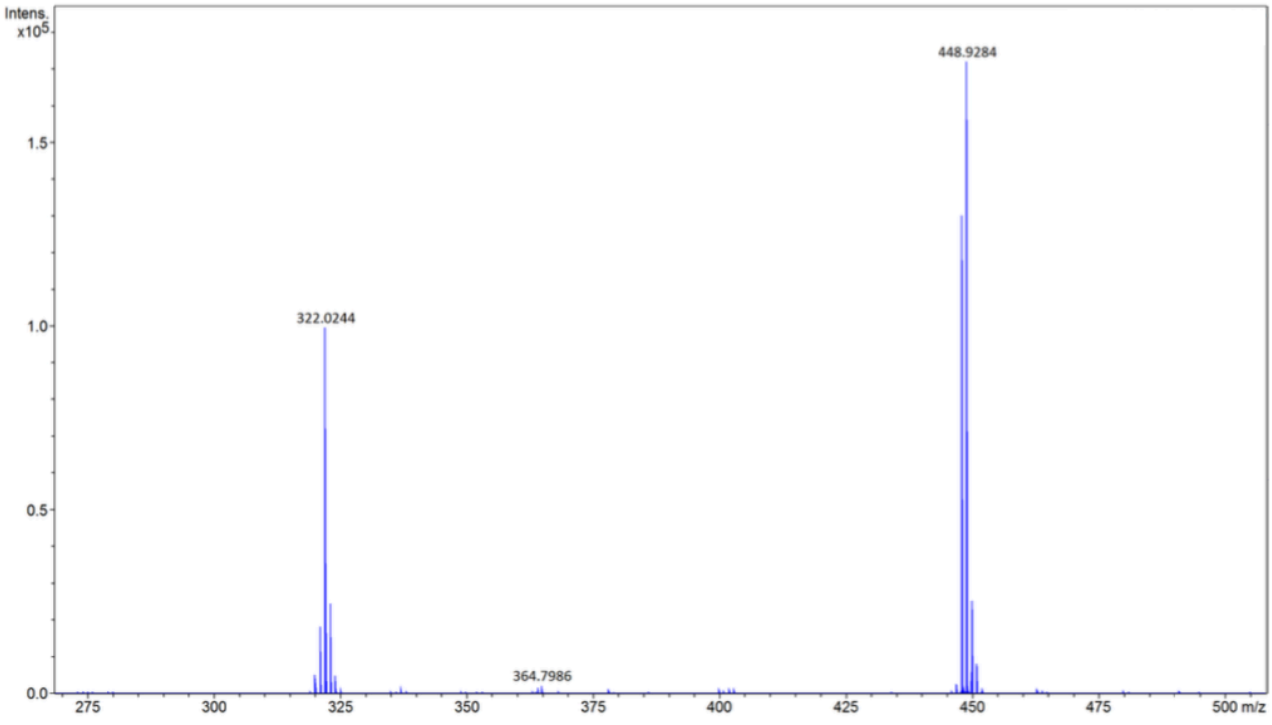

Figure S16: APCI-MS spectrum of **5**

Characterization of **P1**

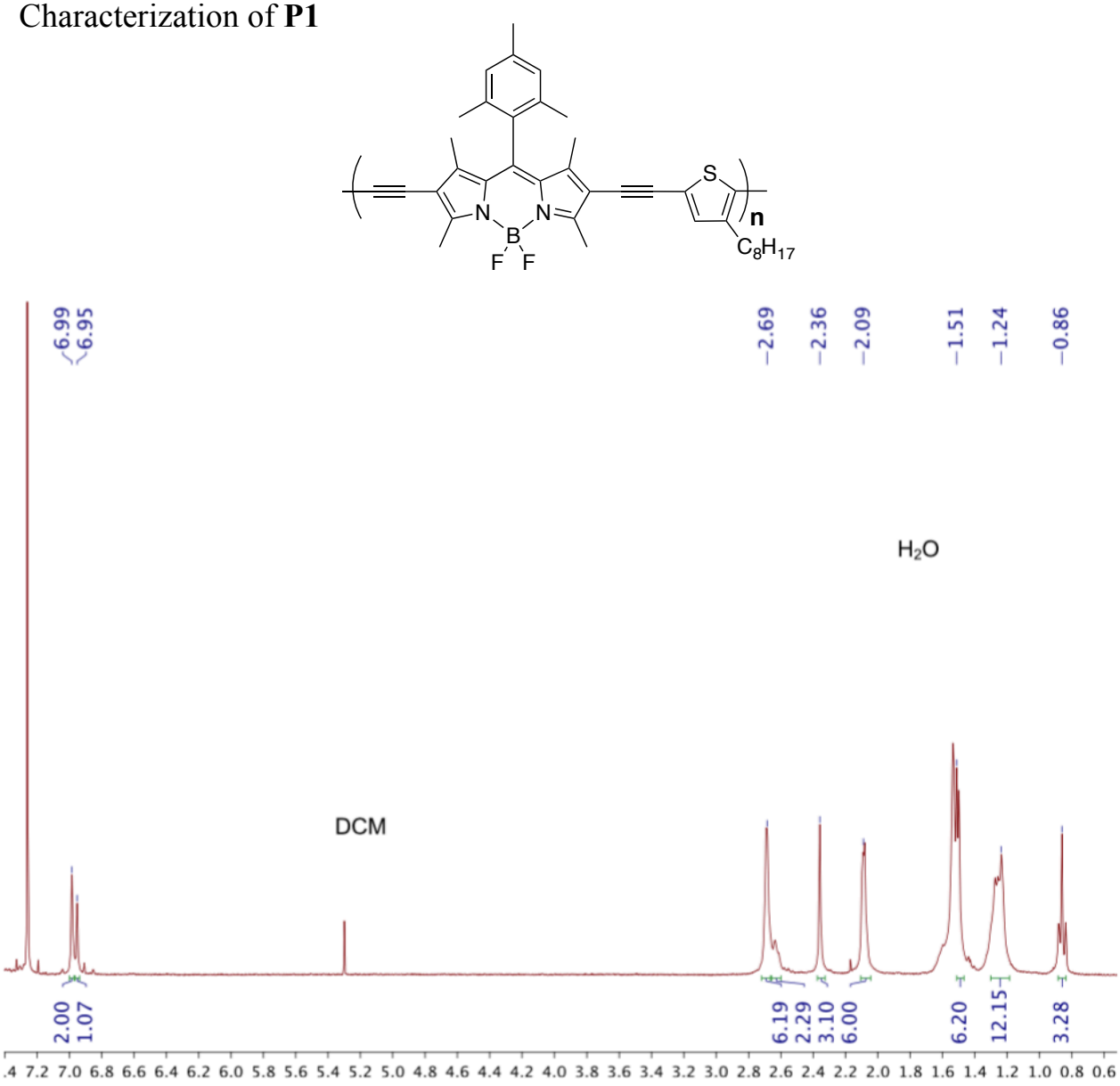

Figure S17: ^{1}H NMR spectrum of **P1** (300 MHz, $CDCl_3$, δ ppm)

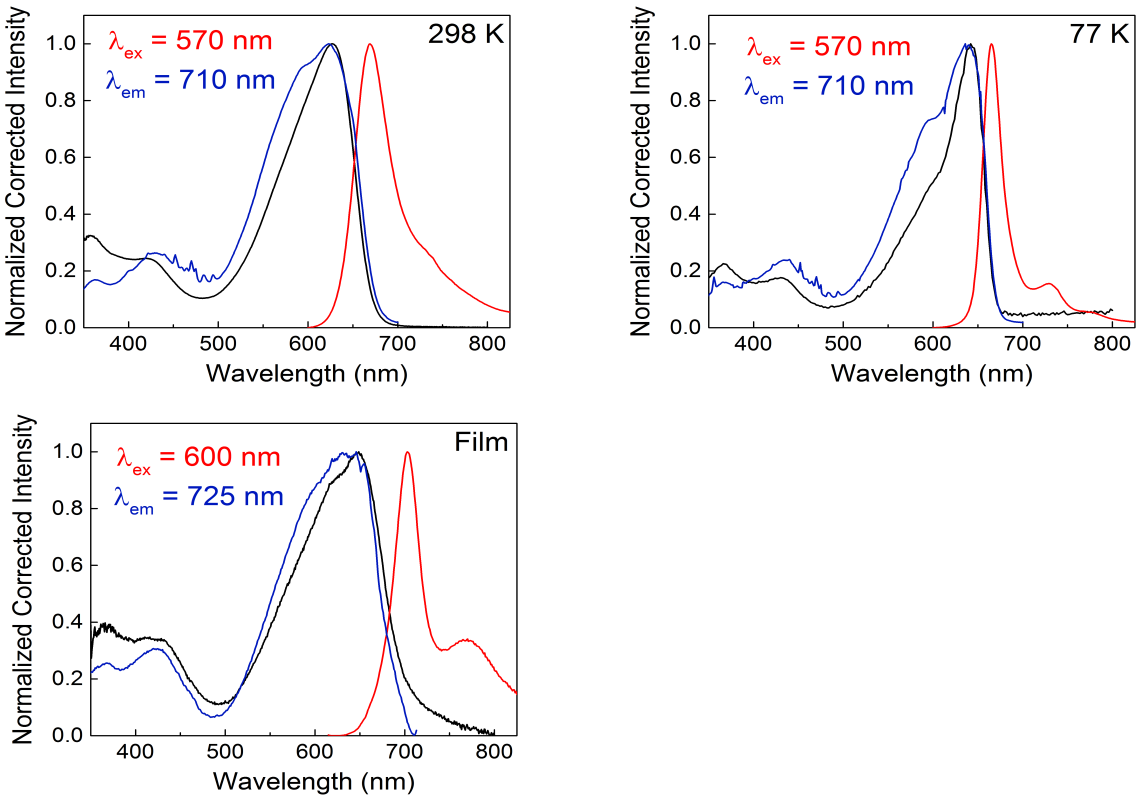

Figure S18: Absorption (black), emission (red), excitation (blue) of **P[BdP-OT] P1** at 298 K and 77 K in 2-MeTHF and in thin film

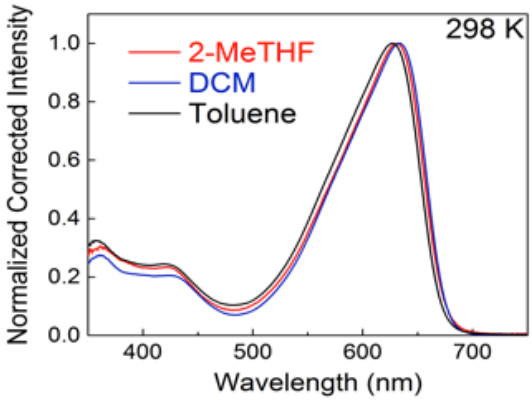

Figure S19: Absorption spectra of **P[BdP-OT] P1** in 2-MeTHF (red), DCM (blue) and toluene (black) at 298 K

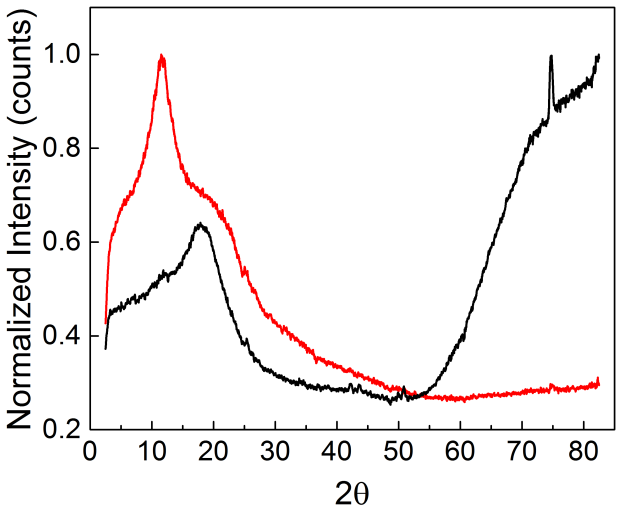

Figure S20: Films DRX before (black) and after (red) thermal annealing (100 °C, 10 min)

Characterization of **P2**

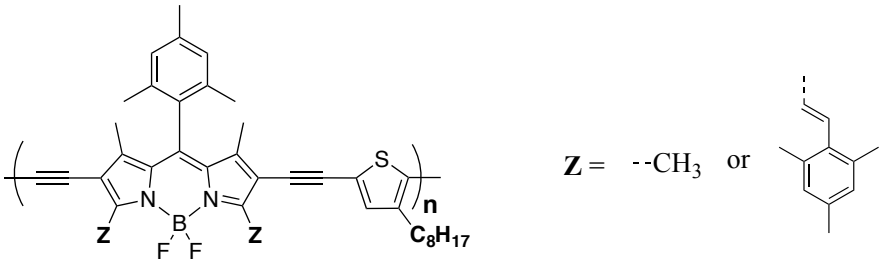

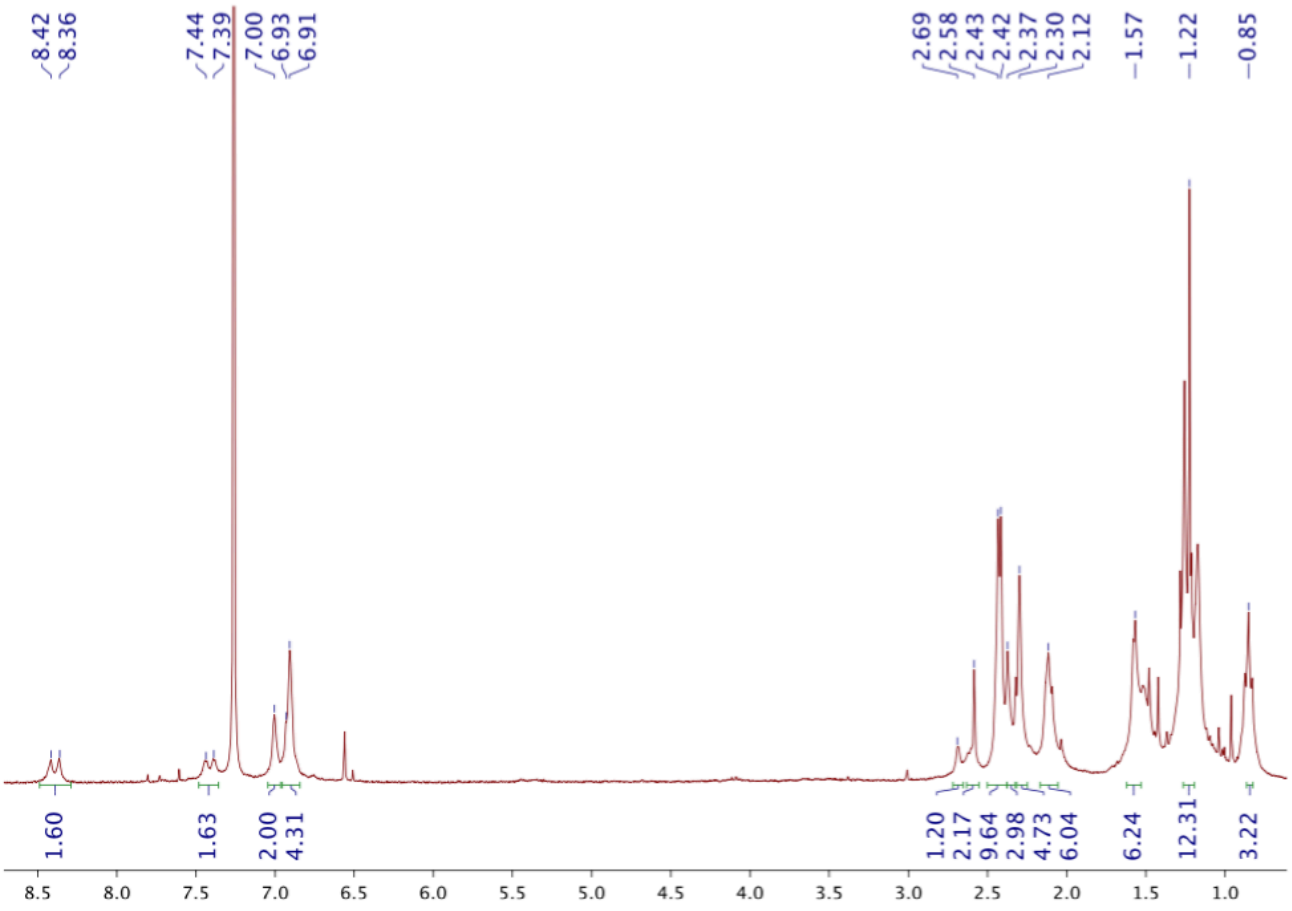

Figure S21: ^{1}H NMR spectrum of **P2** (300 MHz, $CDCl_3$, δ ppm)

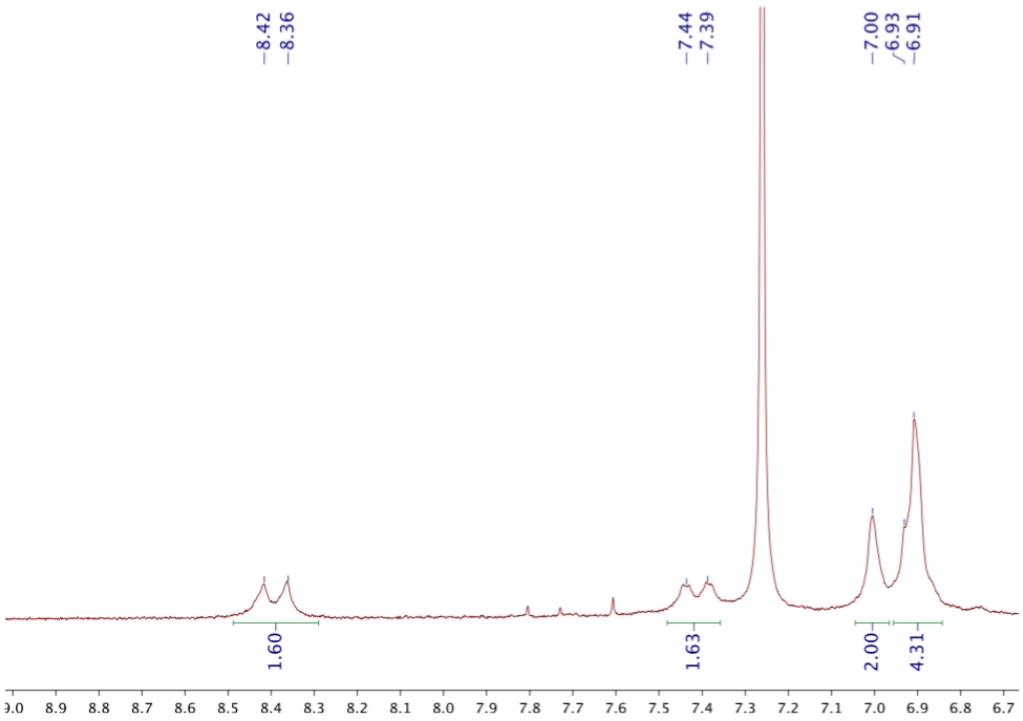

Figure S22: ^{1}H NMR of **P2** spectrum (300 MHz, $CDCl_3$, δ ppm) – Zoom on aromatic region

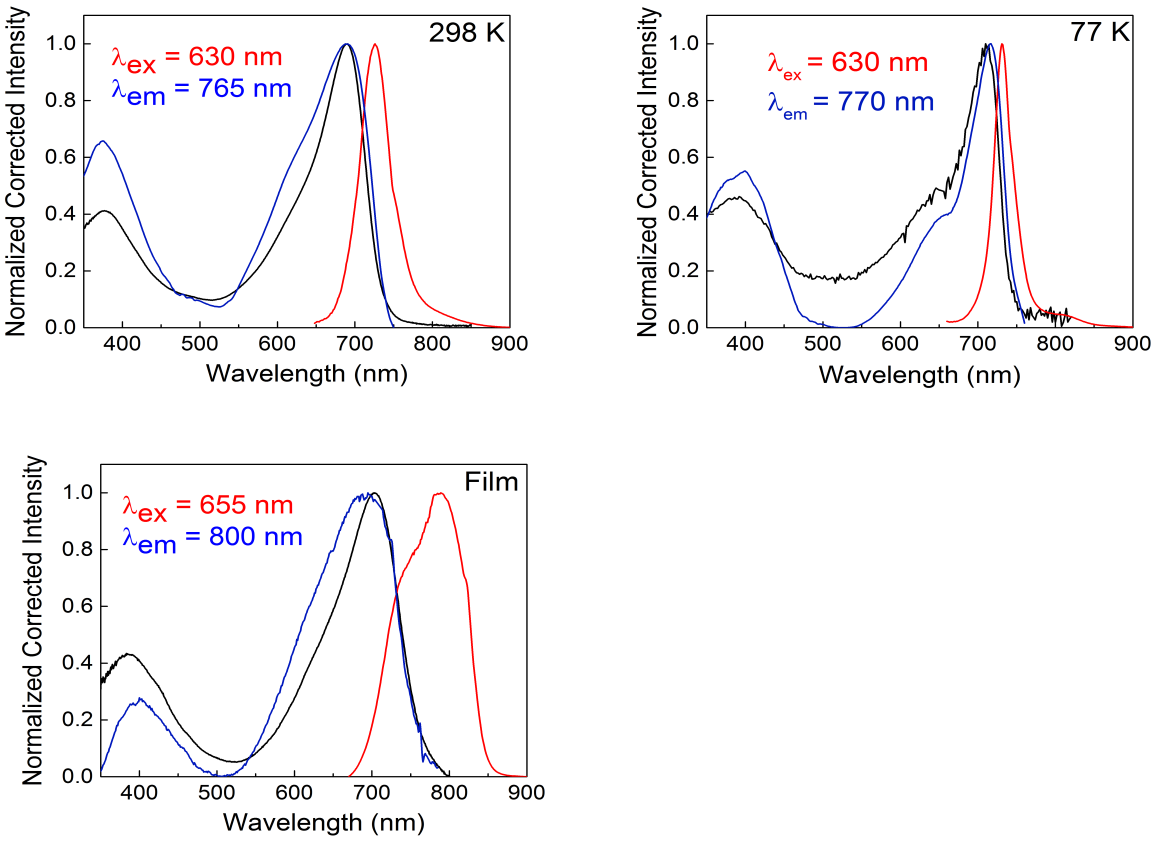

Figure S23: Absorption (black), emission (red), excitation (blue) of **P[sBdP-OT] P2** at 298 K and 77 K in 2-MeTHF and in thin film

Thermal properties of **P1** and **P2**.

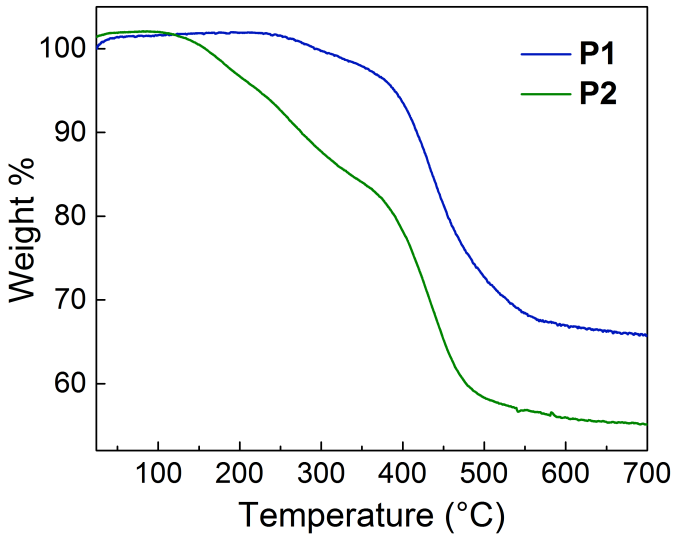

Figure S24: TGA thermograms of **P1** and **P2 -** Experiments were performed under Argon at a heating rate of 10 °C.min^{-1}

Characterization of **6**

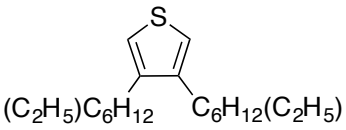

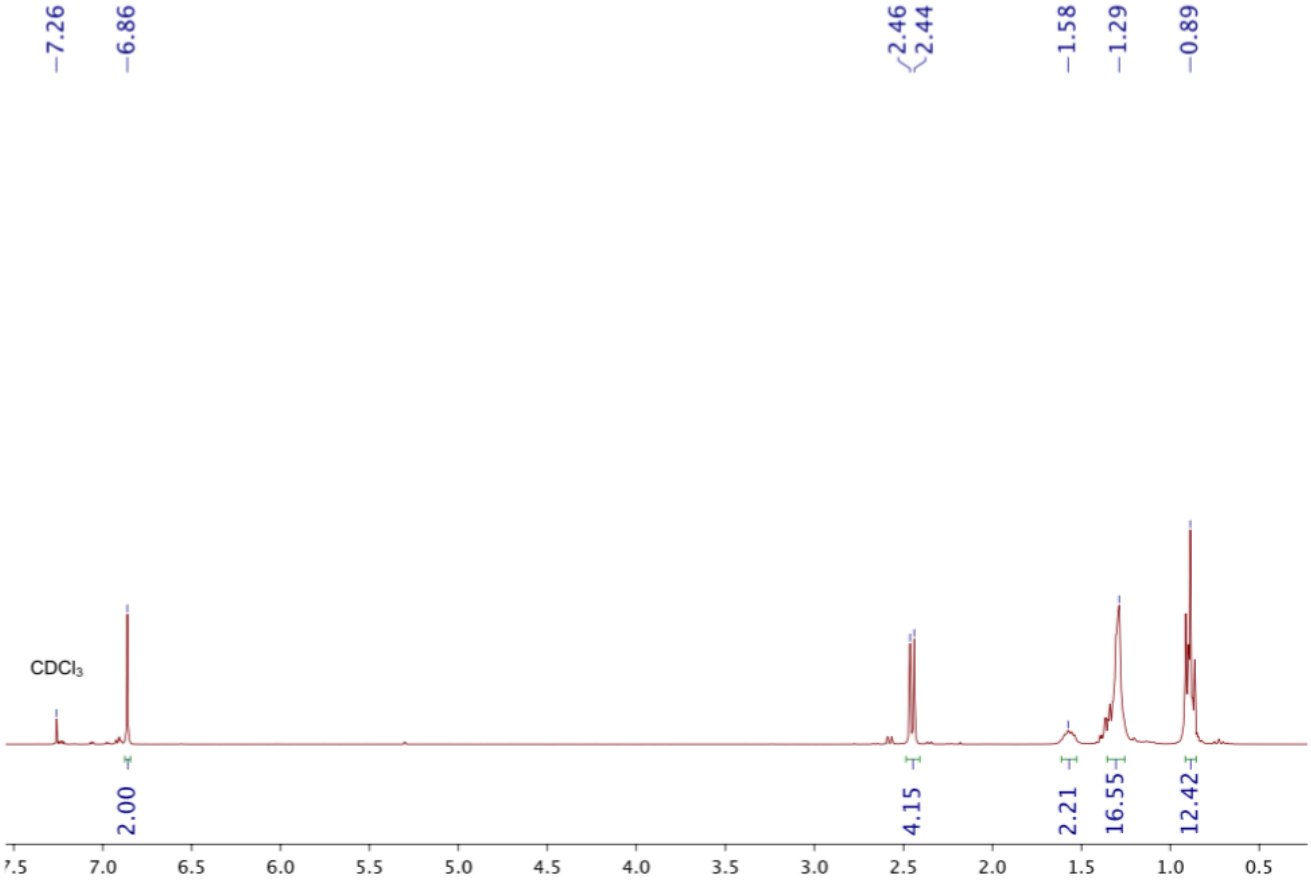

Figure S25: ^{1}H NMR spectrum of **6** (300 MHz, $CDCl_3$, δ ppm)

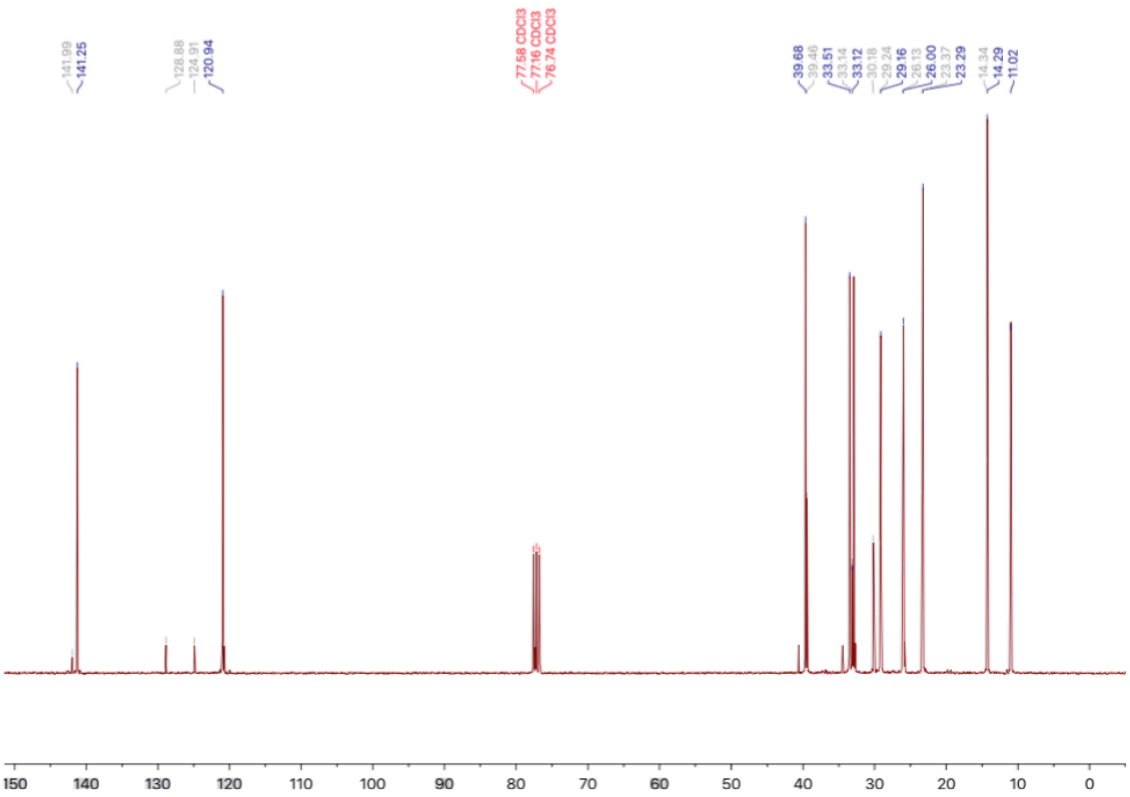

Figure S26: ^{13}C NMR spectrum of **6** (75 MHz, $CDCl_3$, δ ppm)

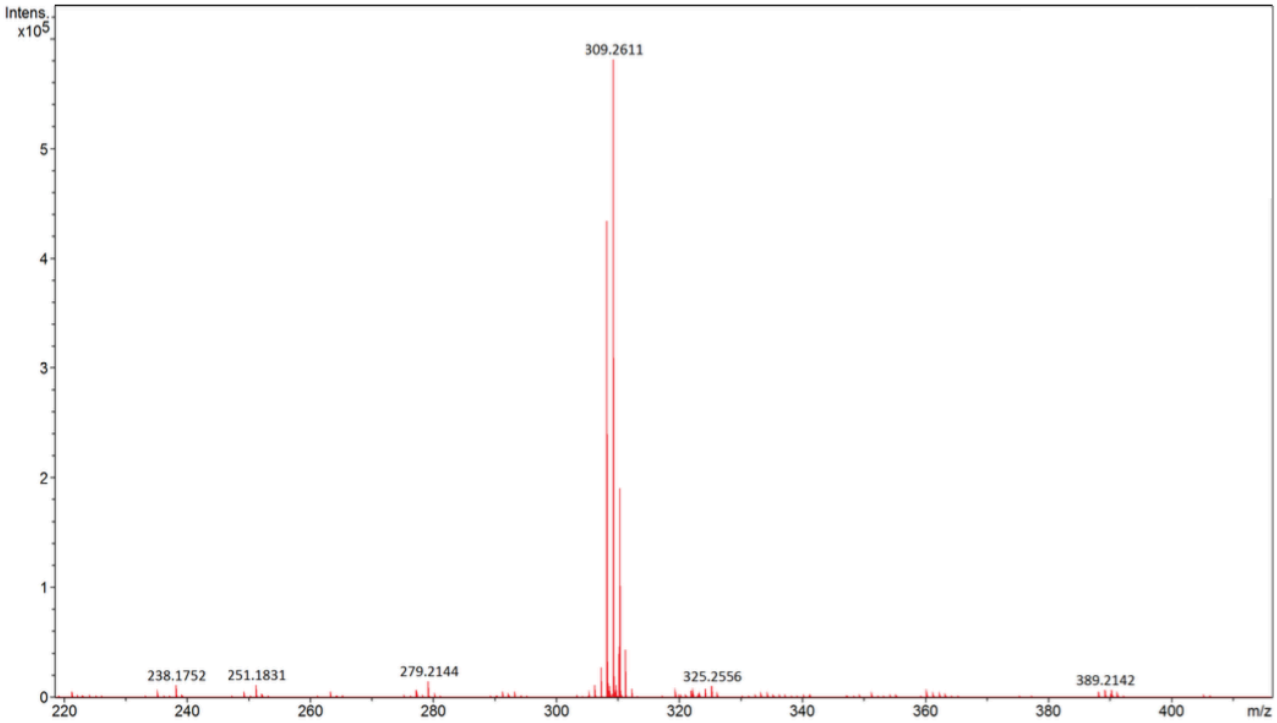

Figure S27: APCI-MS spectrum of **6**

Characterization of **7**

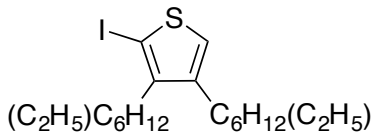

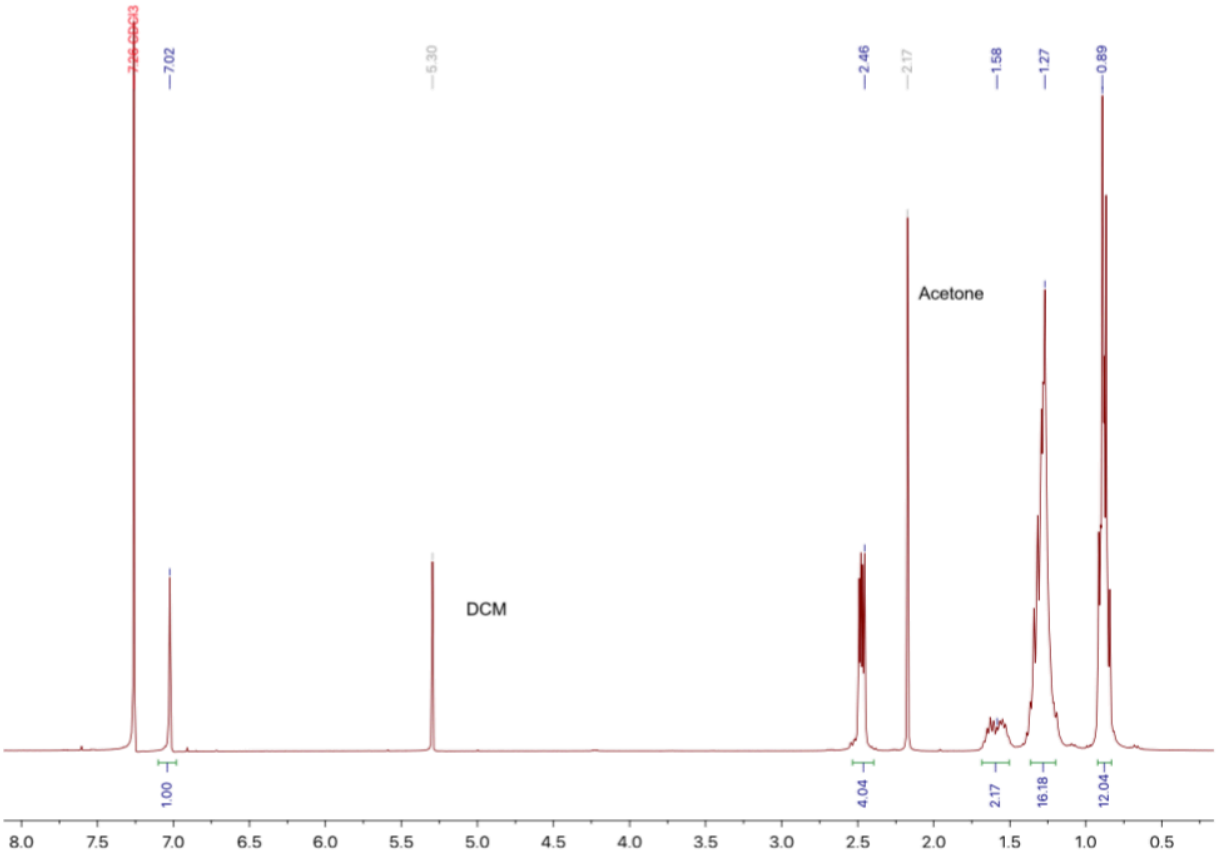

Figure S28: ^{1}H NMR spectrum of **7** (300 MHz, $CDCl_3$, δ ppm)

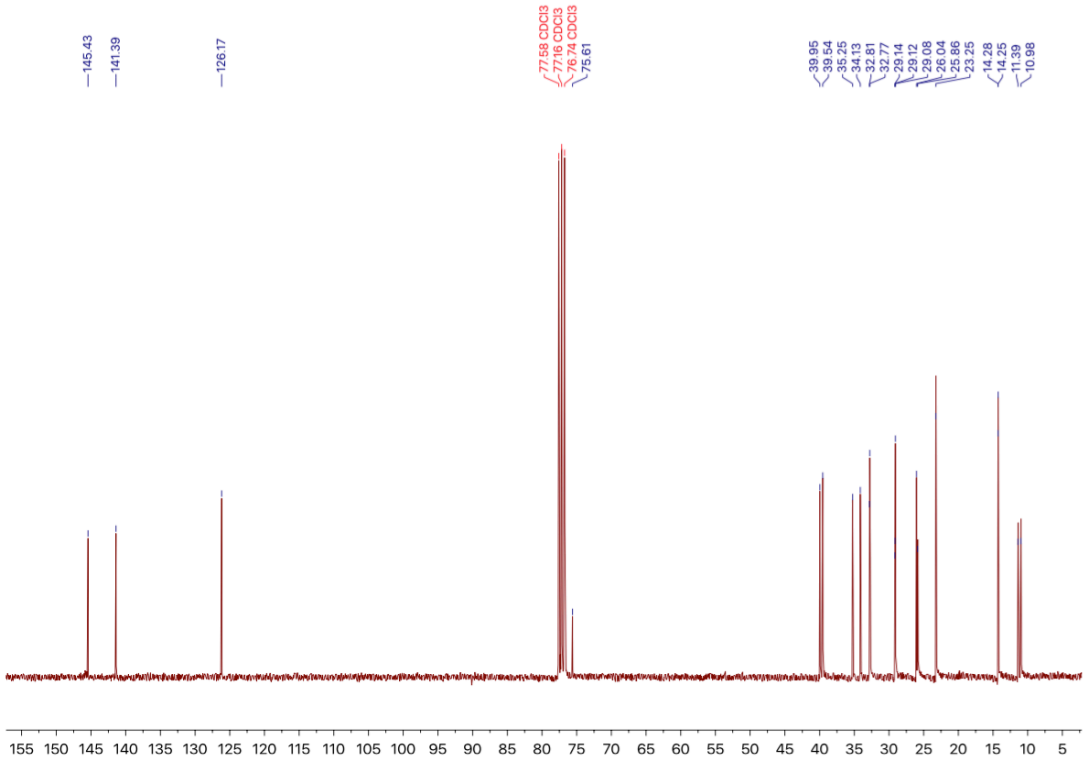

Figure S29: ^{13}C NMR spectrum of **7** (75 MHz, $CDCl_3$, δ ppm)

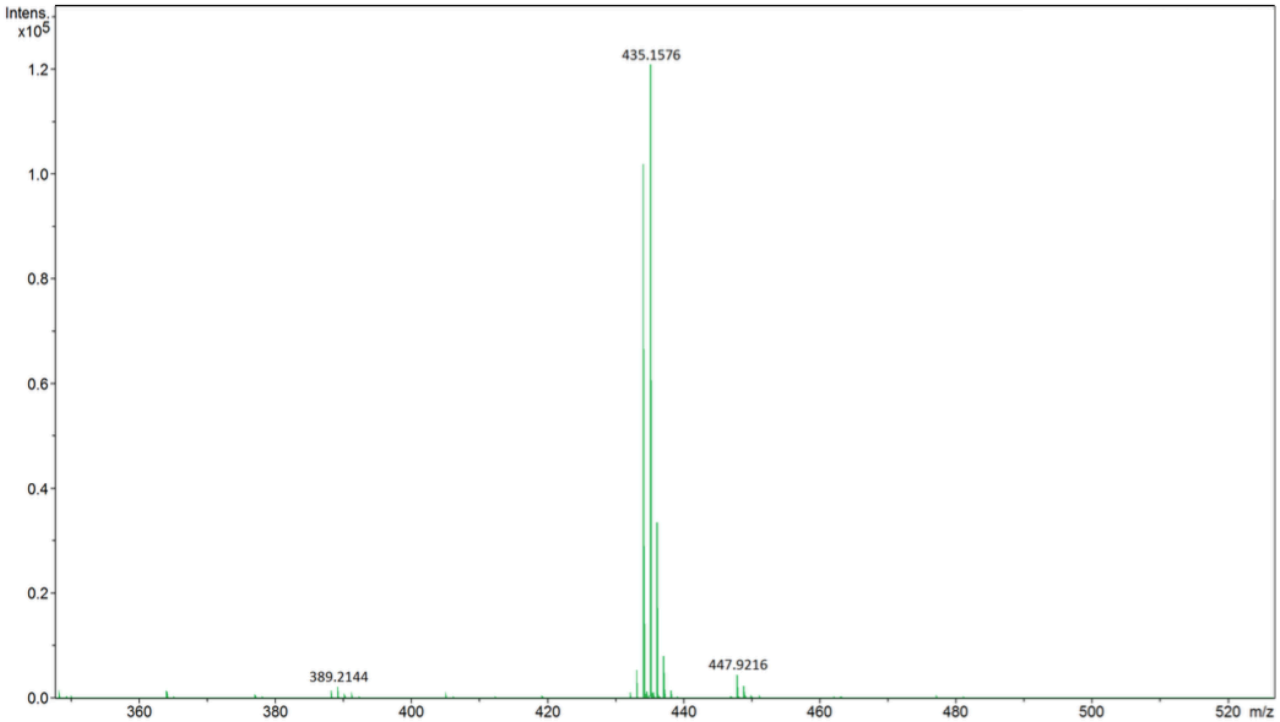

Figure S30: APCI-MS spectrum of **7**

Characterization of **8**

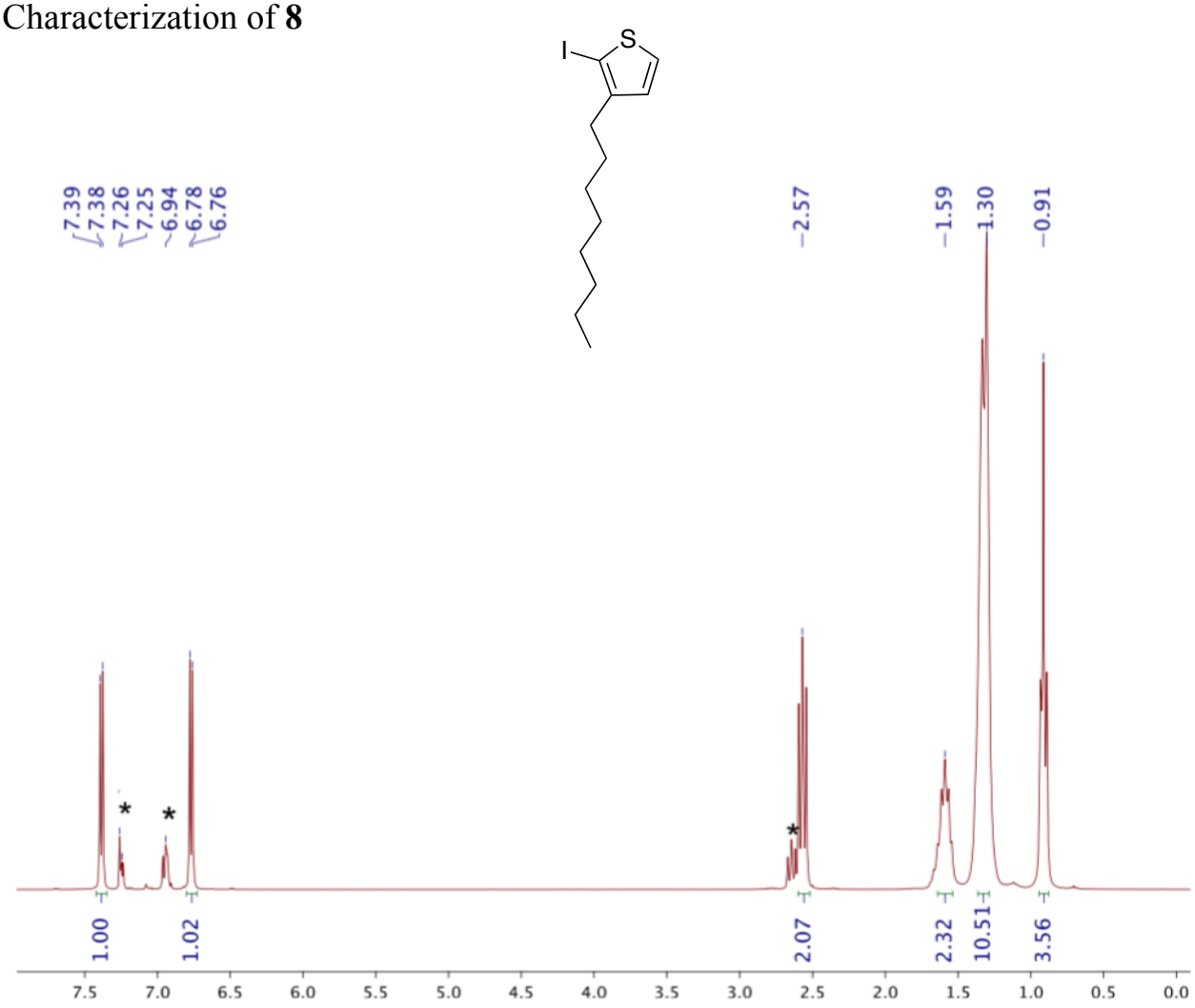

Figure S31: ^{1}H NMR spectrum of **8** (300 MHz, $CDCl_3$, δ ppm)

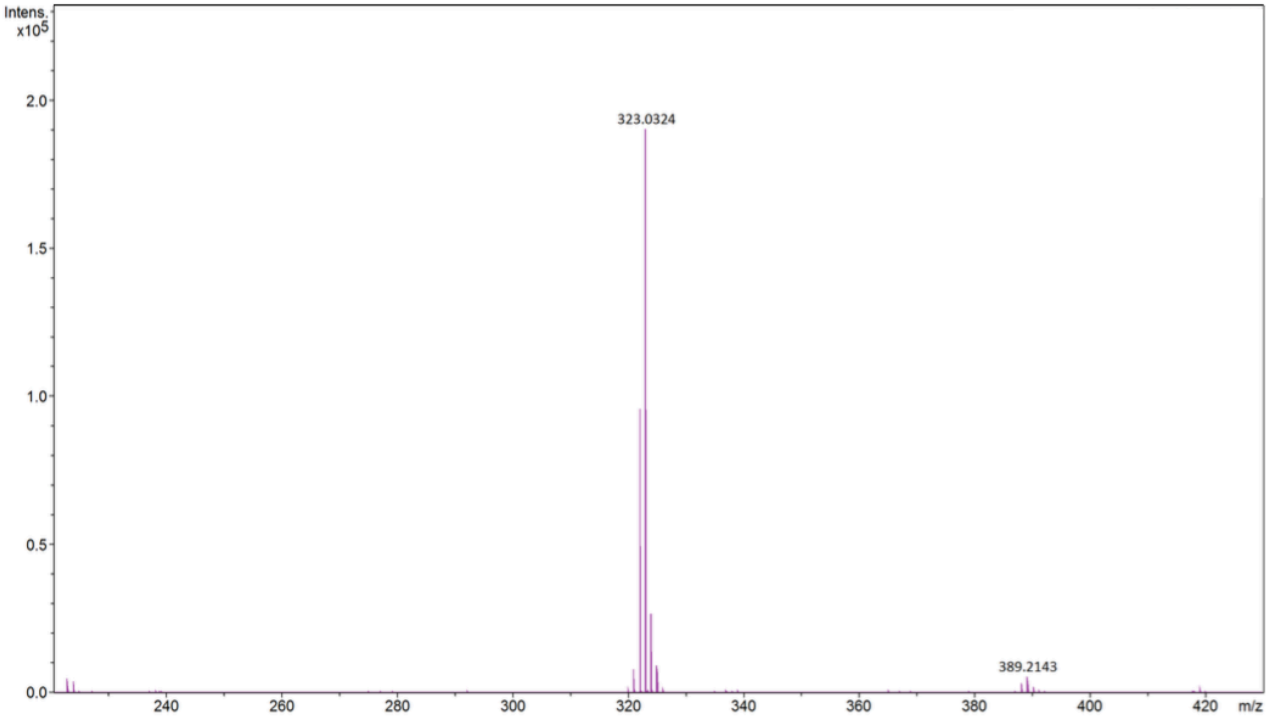

Figure S32: APCI-MS spectrum of **8**

Characterization of **M1**

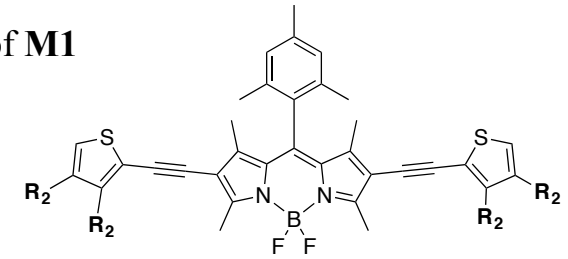

R2 =

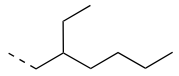

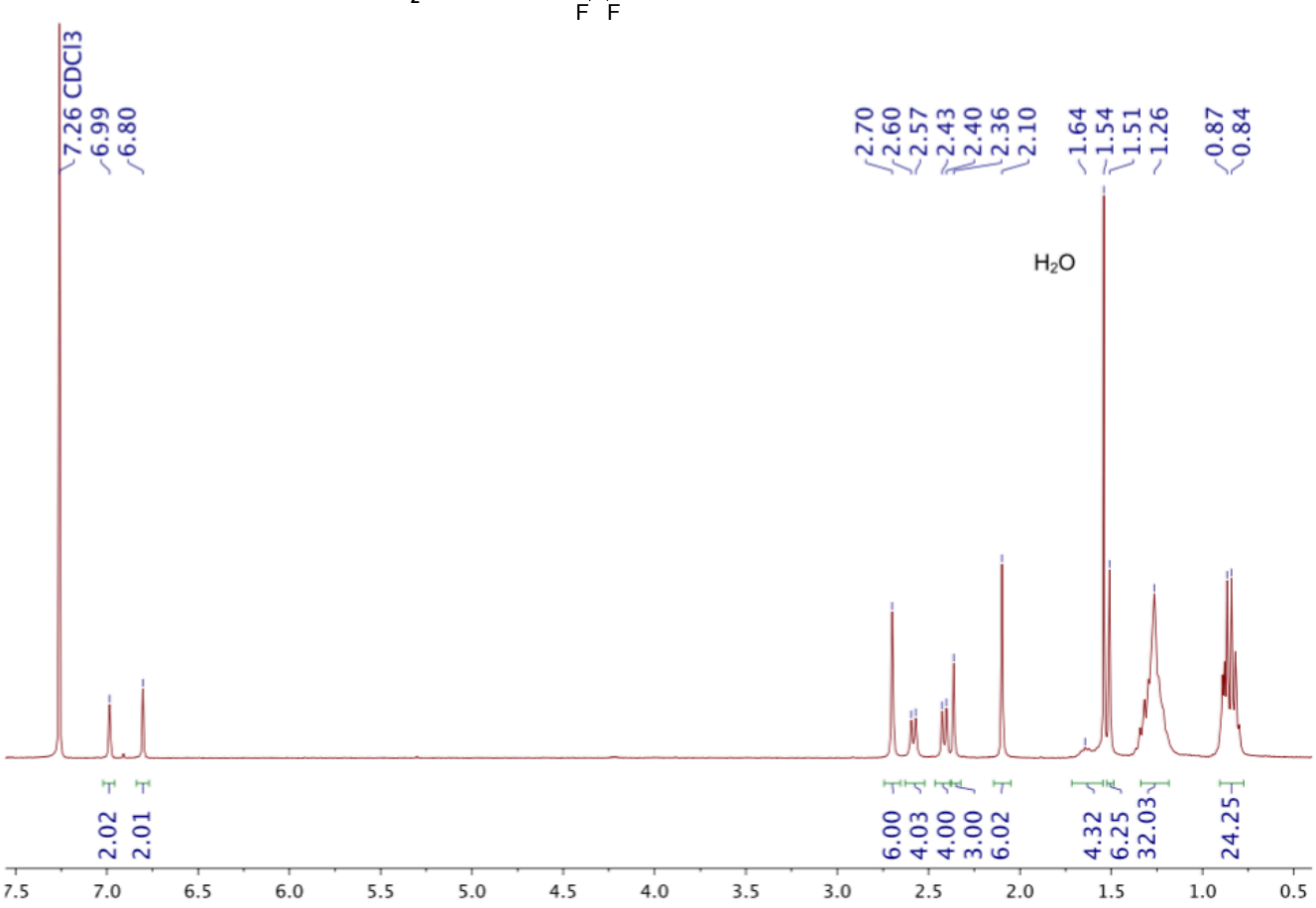

Figure S33: ^{1}H NMR spectrum of **M1** (300 MHz, $CDCl_3$, δ ppm)

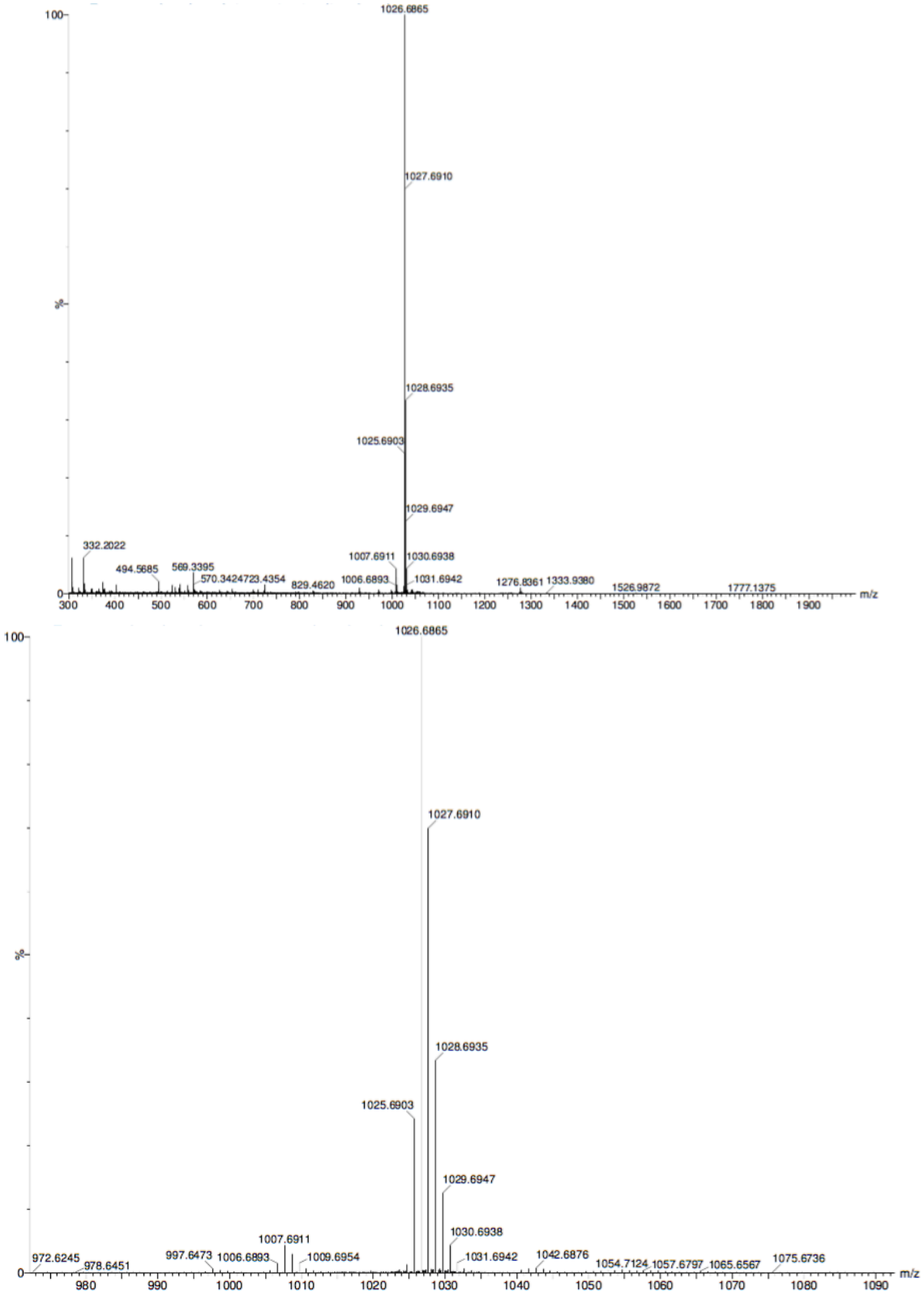

Figure S34: MALDI/TOF-MS full (top) and zoom (bottom) spectrum of **M1**

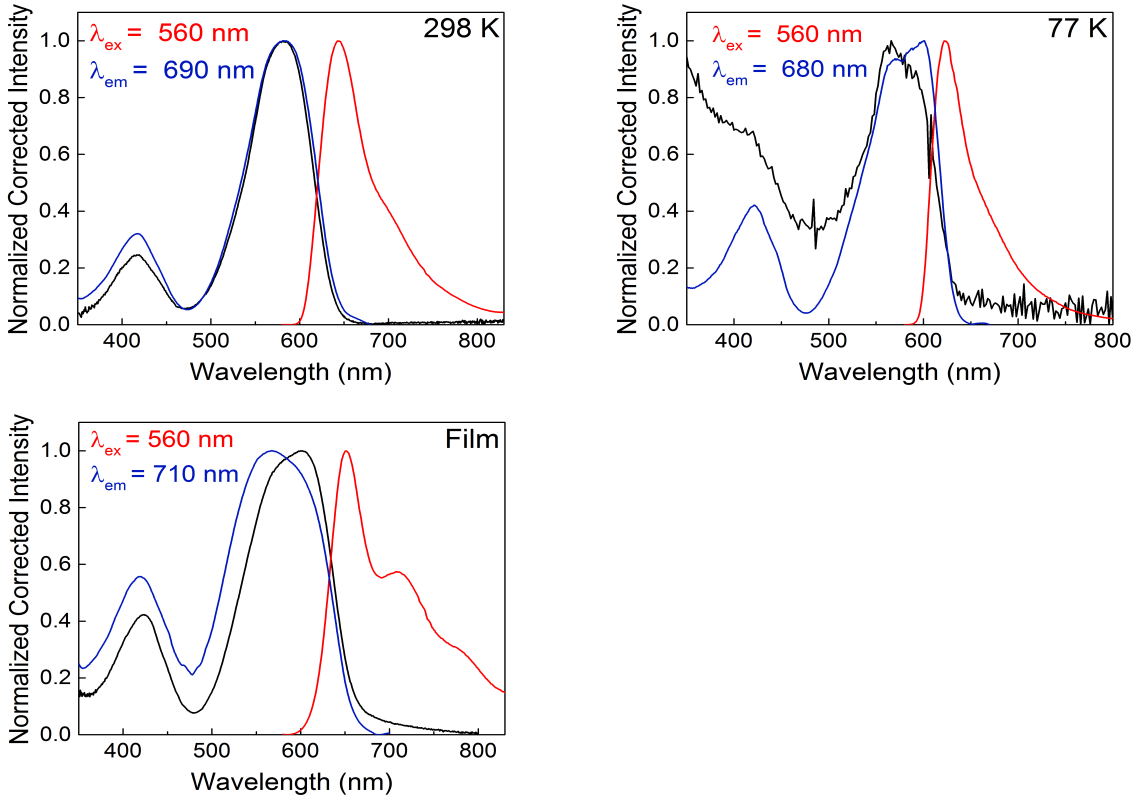

Figure S35: Absorption (black), emission (red), excitation (blue) of **M1** at 298 K, 77 K in 2-MeTHF and in thin film

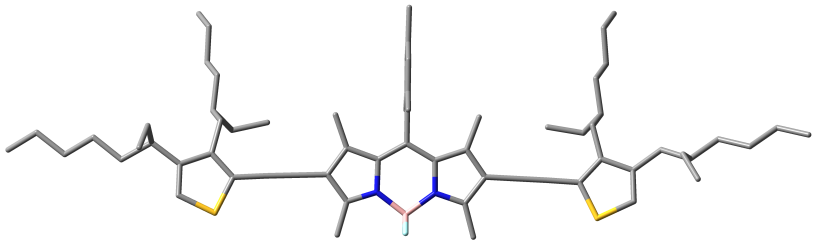

Figure S36: Optimized geometry (DFT, B3LYP) for **M1**

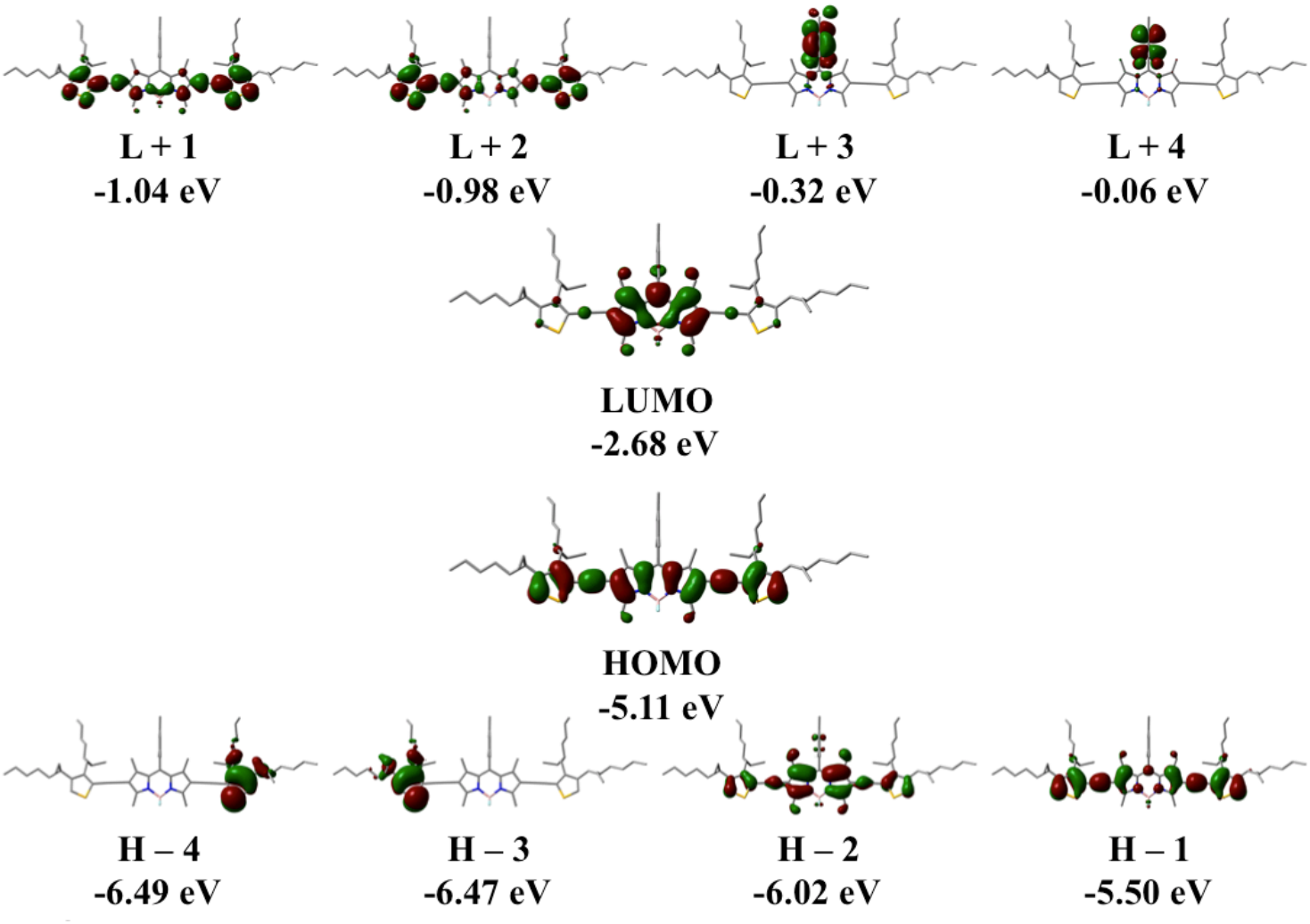

Figure S37: Representations of the frontier MOs for **M1** with corresponding energies

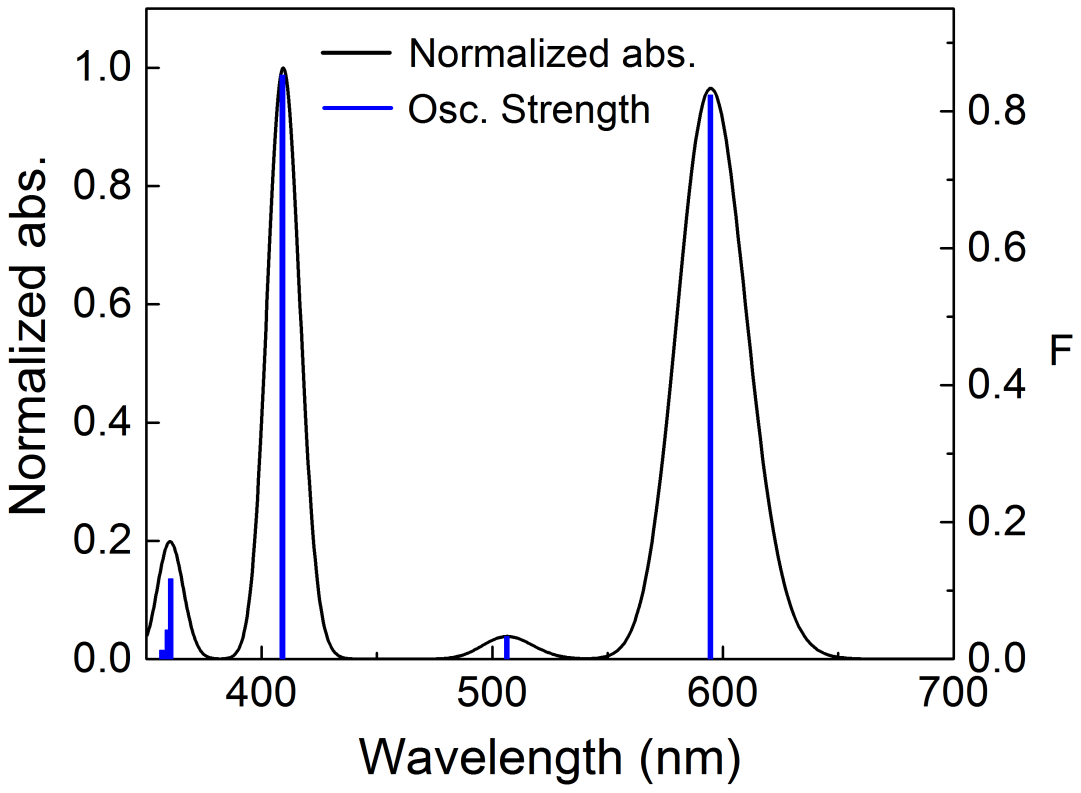

Figure S38: Computed oscillator strength (F) as a function of the calculated positions of the first 75 electronic transitions for **M1**

Characterization of **M2**

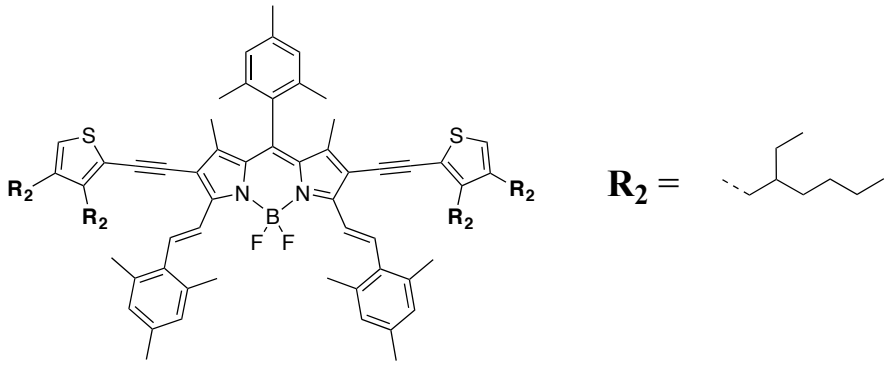

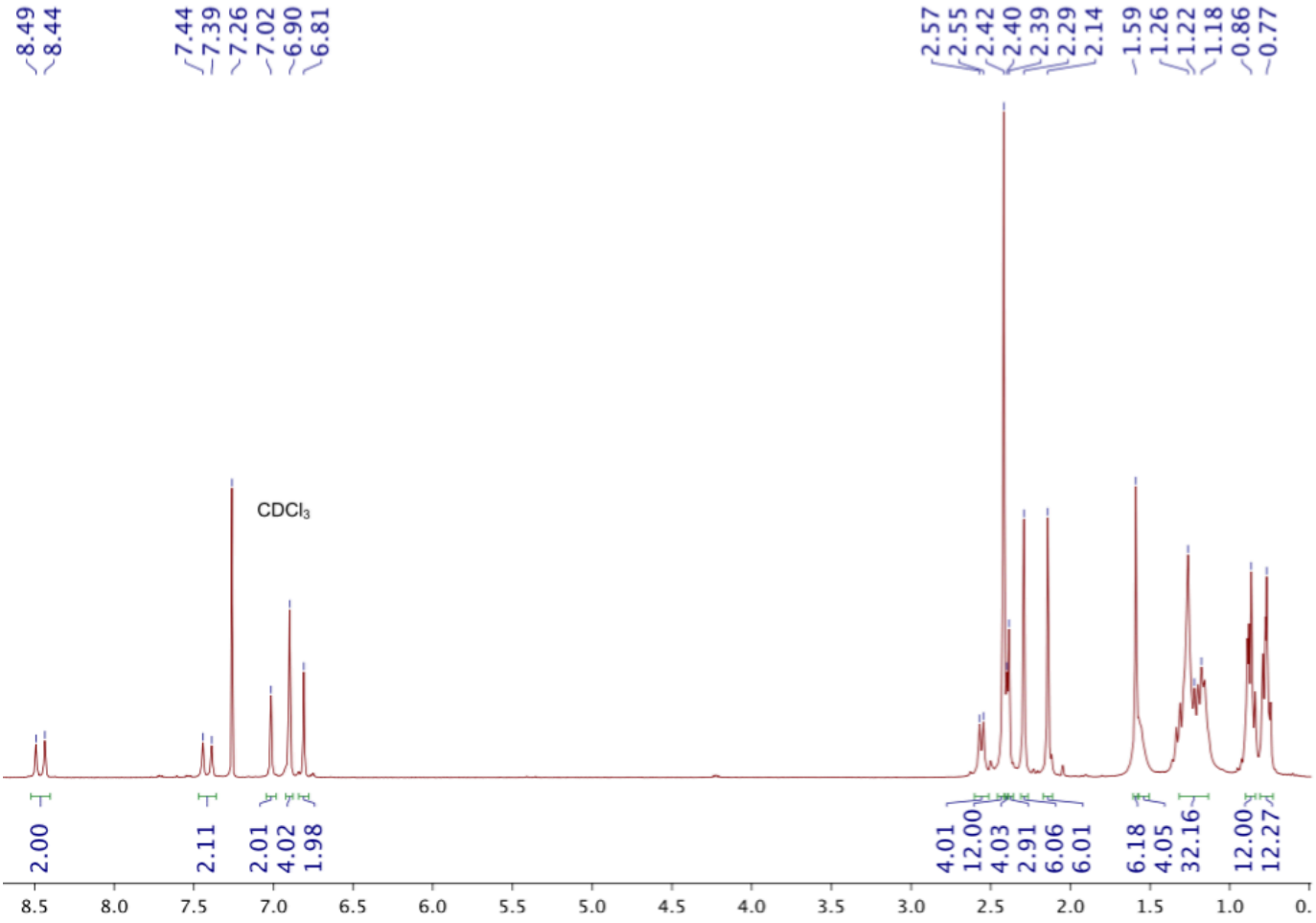

Figure S39: ^{1}H NMR spectrum of **M2** (300 MHz, $CDCl_3$, δ ppm)

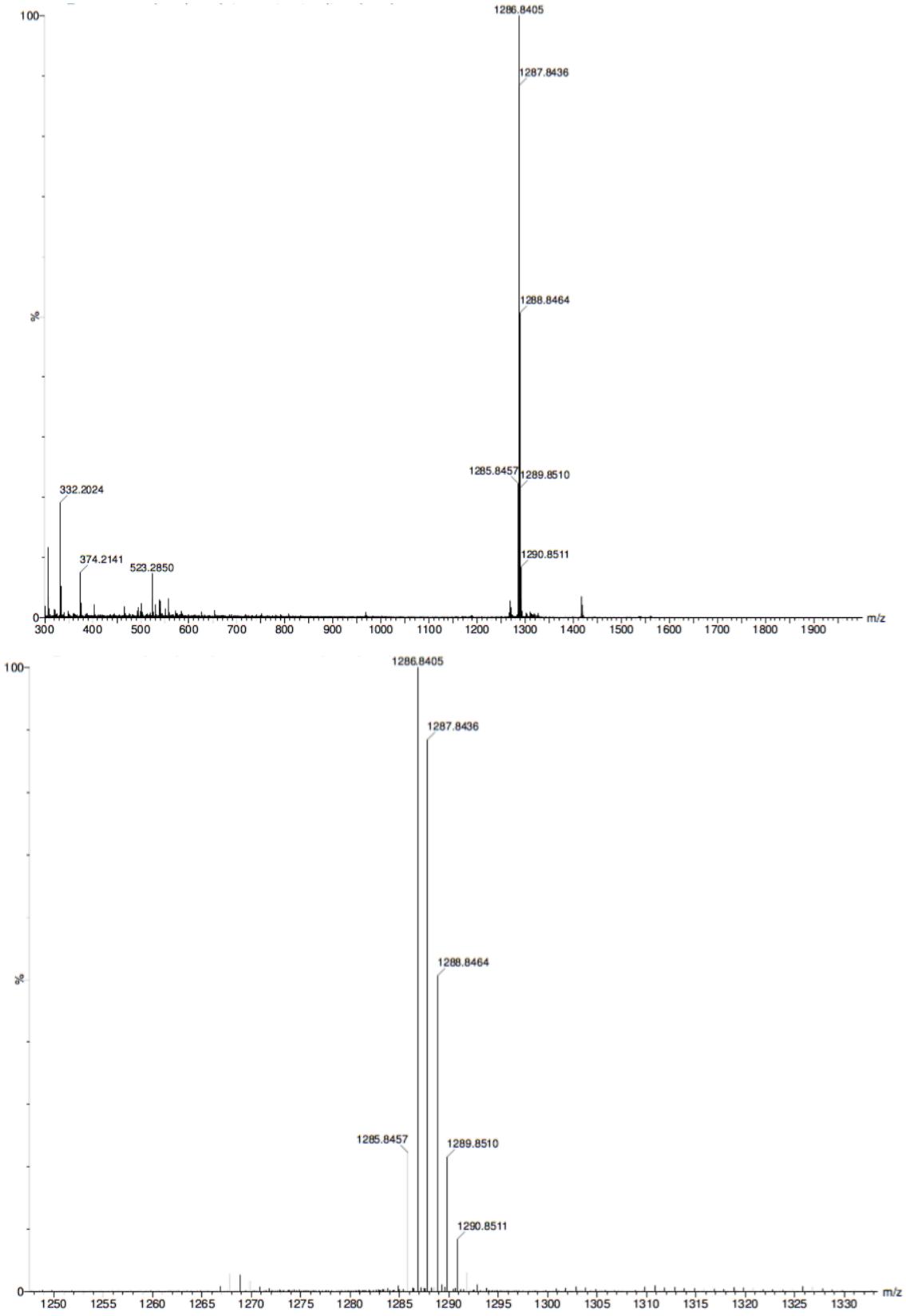

Figure S40: MALDI/TOF-MS full (top) and zoom (bottom) spectra of **M2**

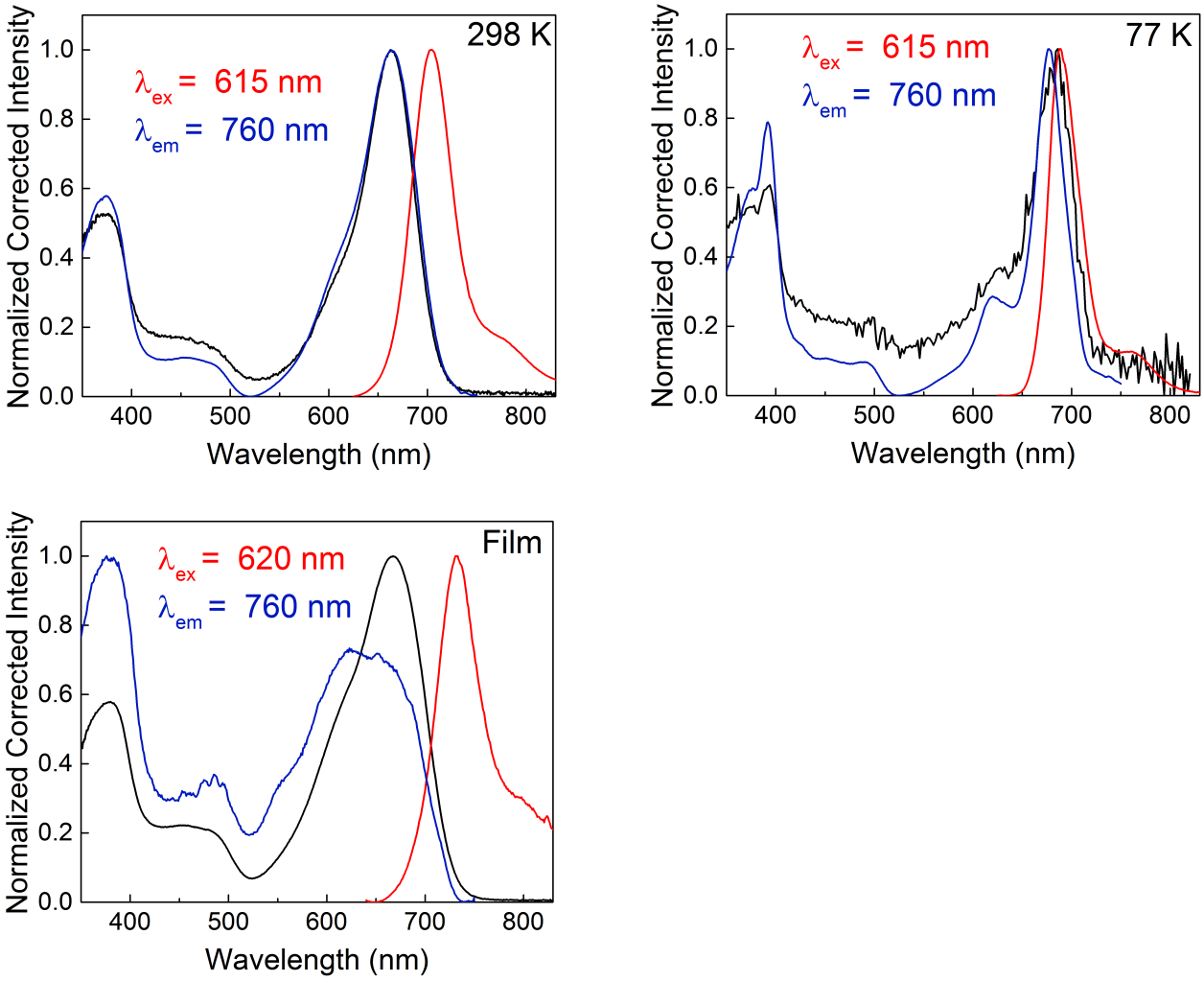

Figure S41: Absorption (black), emission (red), excitation (blue) of **M2** at 298 K, 77 K in 2-MeTHF and in thin film

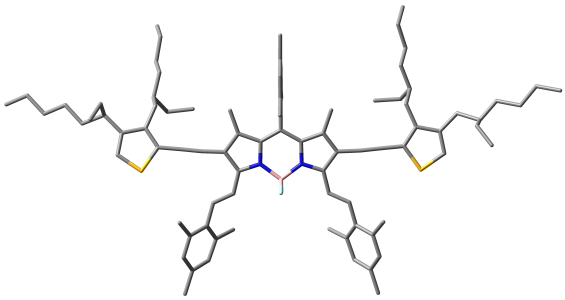

Figure S42: Optimized geometry (DFT, B3LYP) for **M2**

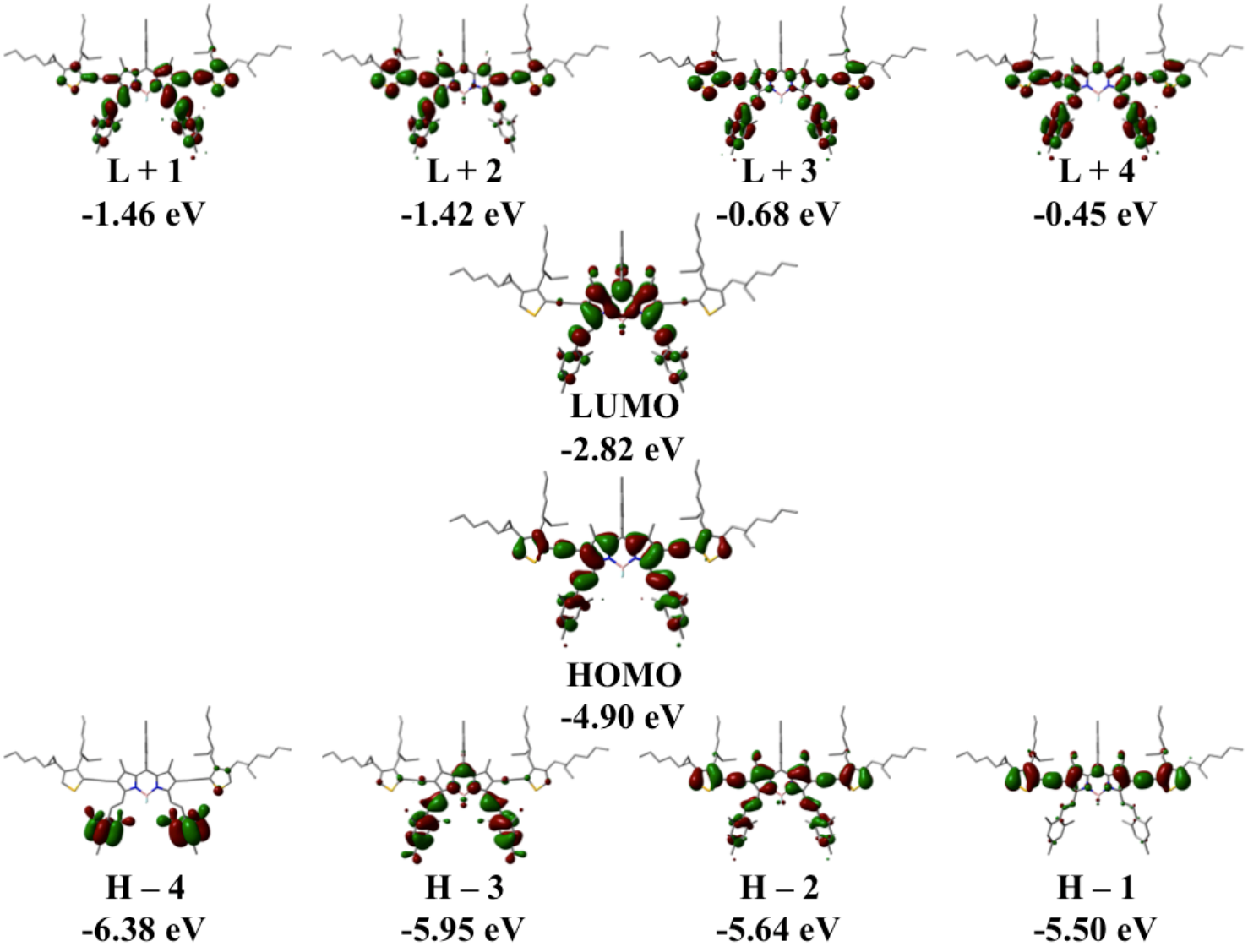

Figure S43: Representations of the frontier MOs for **M2** with corresponding energies

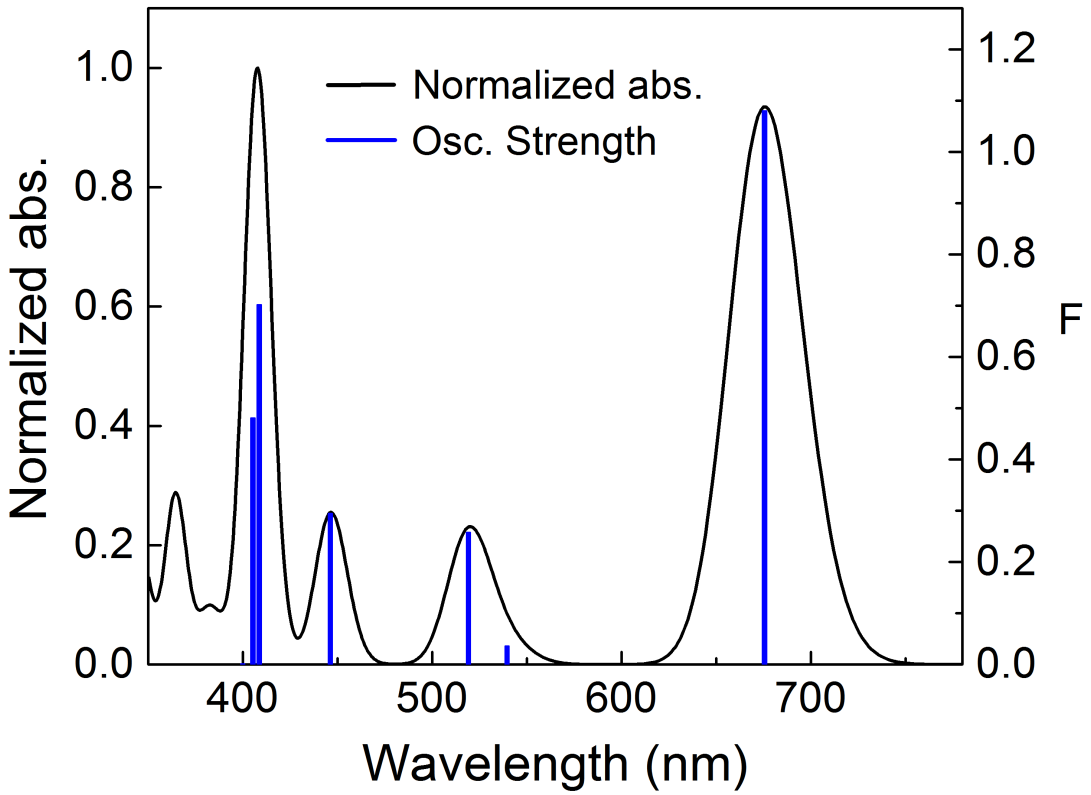

Figure S44: Computed oscillator strength (F) as a function of the calculated positions of the first 75 electronic transitions for **M2**

Characterization of **9**

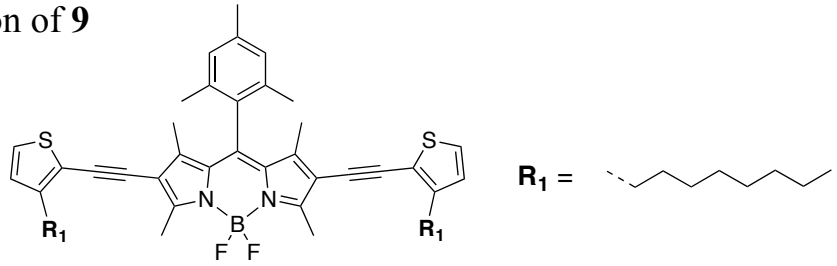

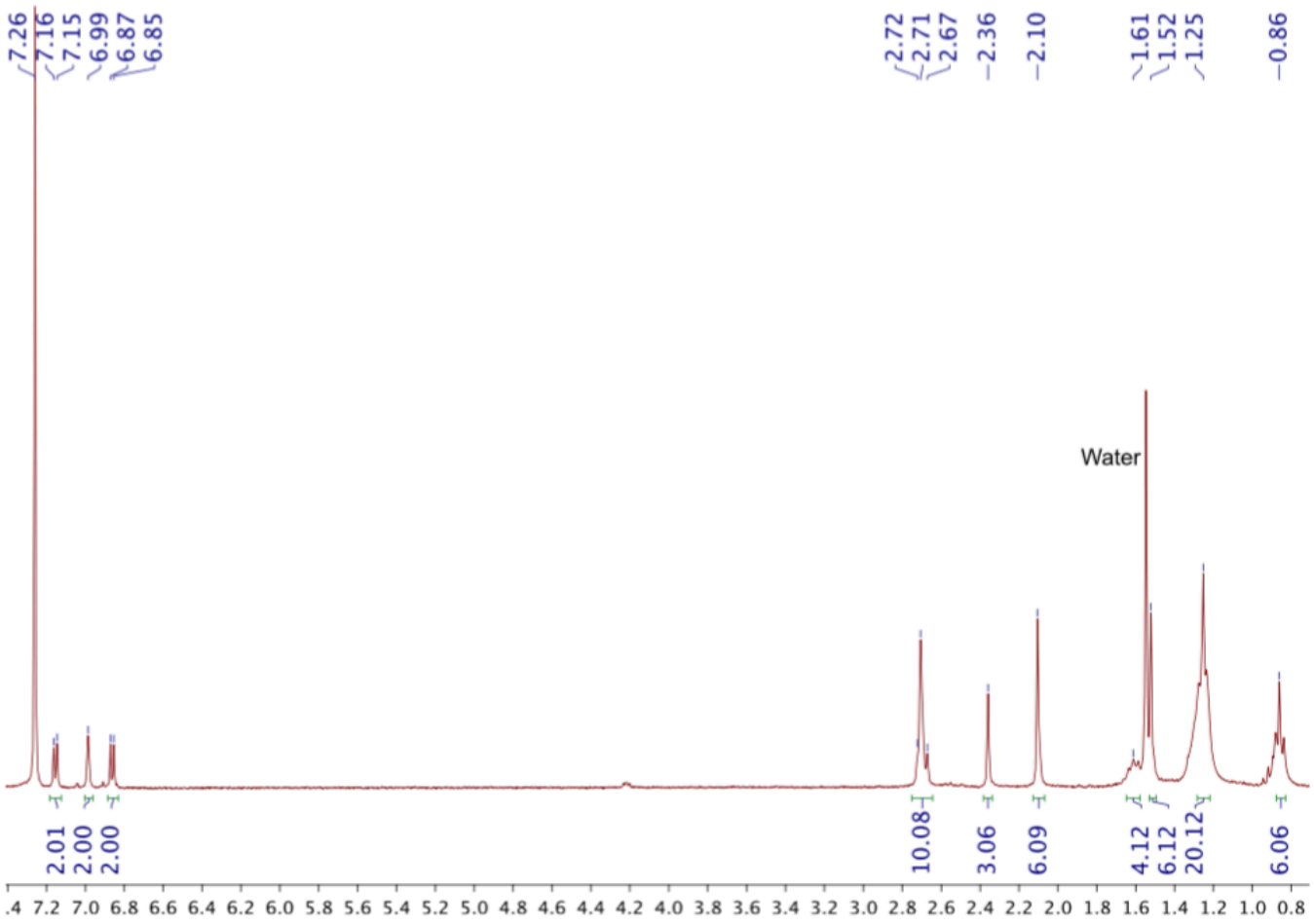

Figure S45: ^{1}H NMR spectrum of **9** (300 MHz, $CDCl_3$, δ ppm)

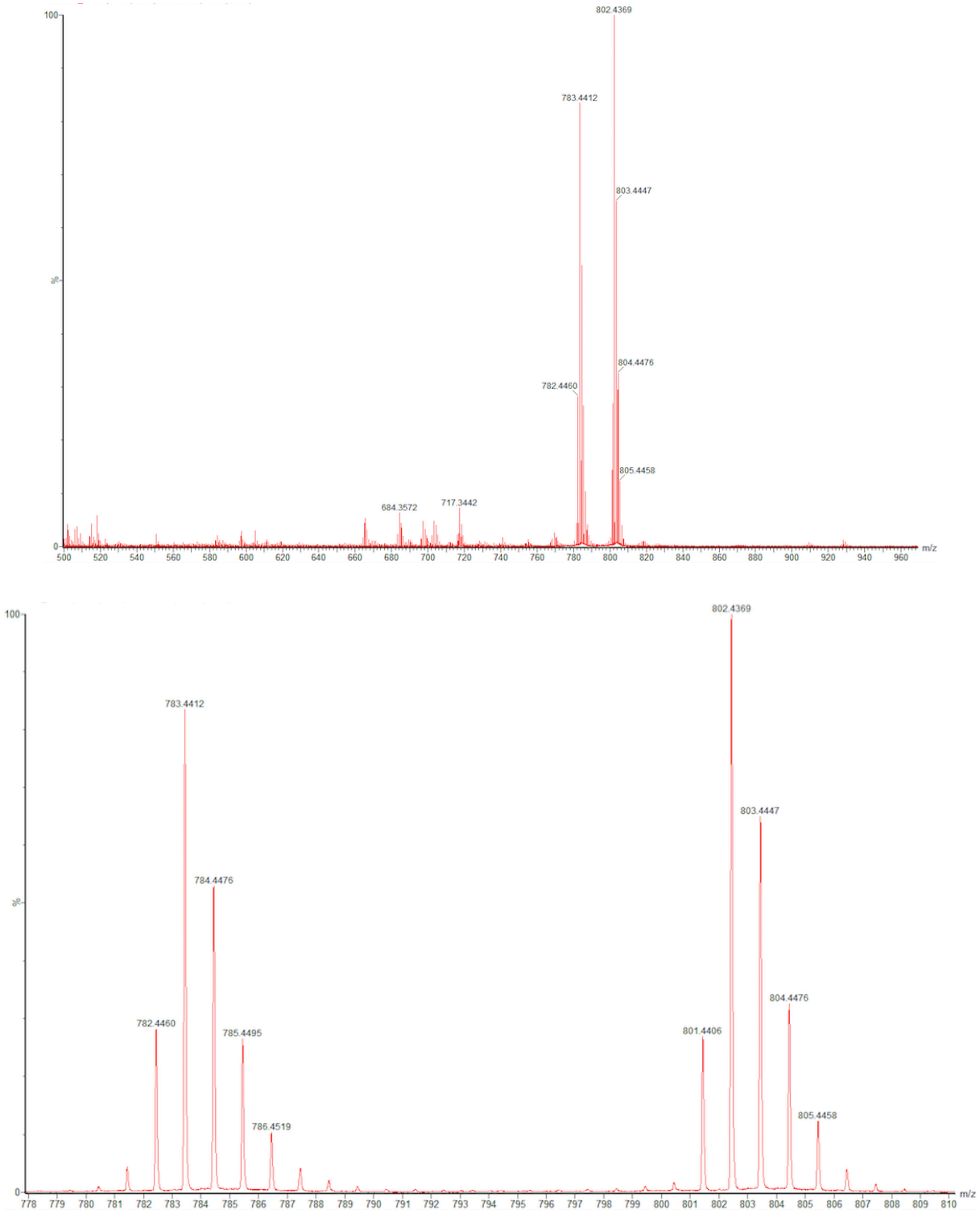

Figure S46: MALDI/TOF-MS full (top) and zoom (bottom) spectra of **9**

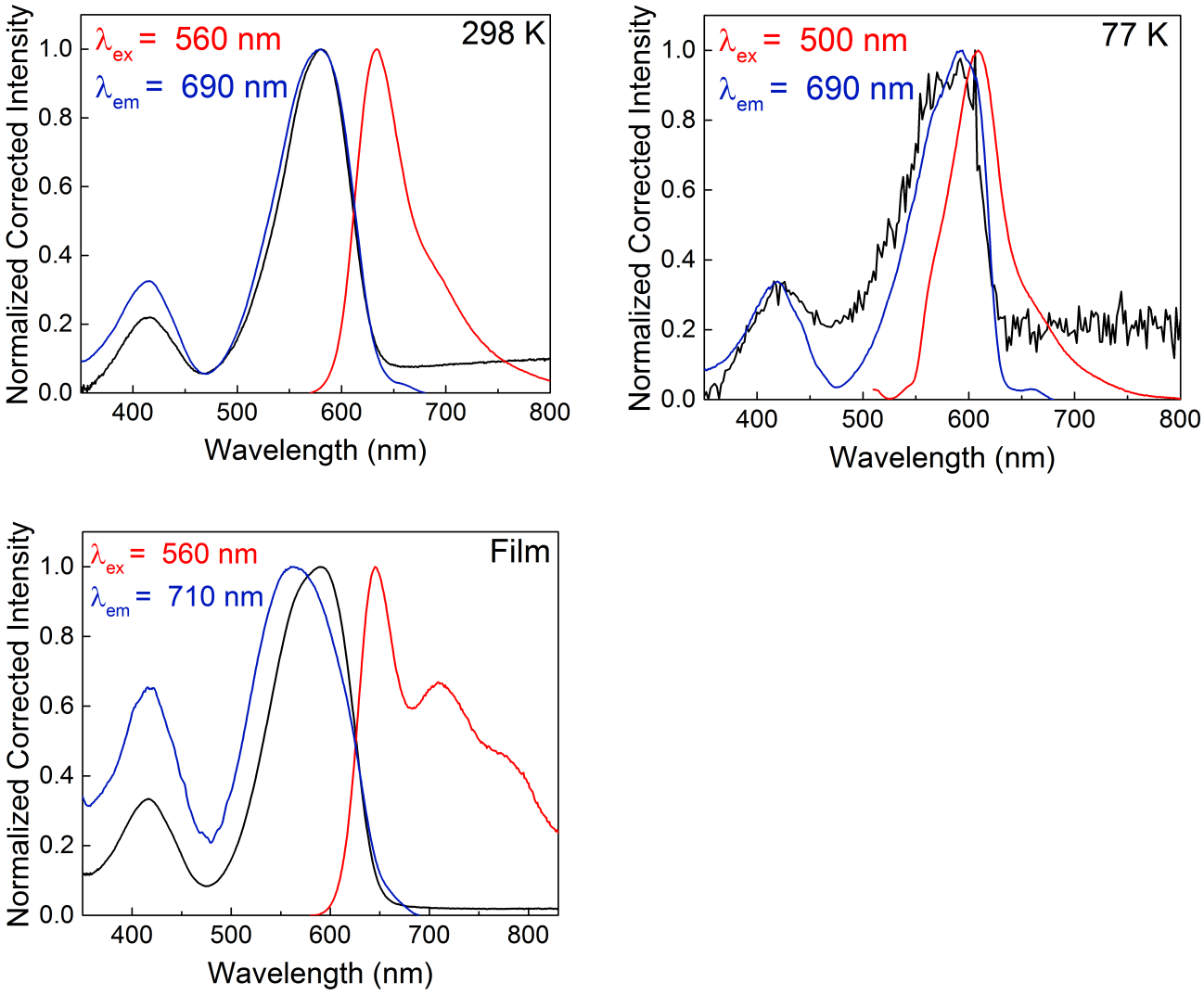

Figure S47: Absorption (black), emission (red), excitation (blue) of **9** at 298 K, 77 K in 2-MeTHF and in thin film

Comparison between **M1** and **9**

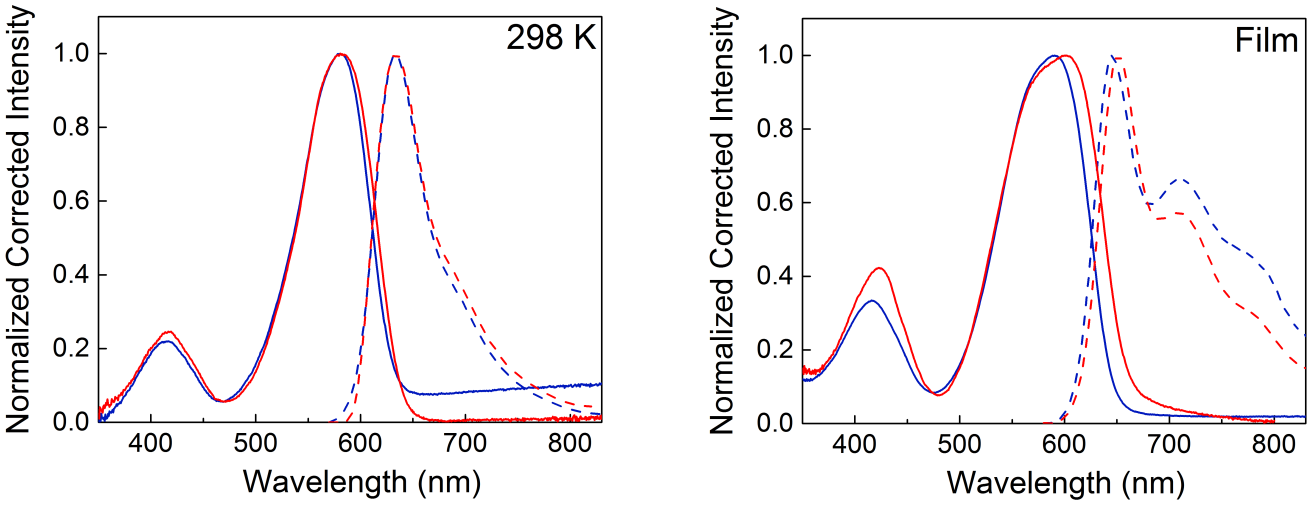

Figure S48: Absorption (solid) and emission (dashed) of **M1** (red) and **9** (blue) at 298 K in 2-MeTHF and in thin film

Table S1: Percent distribution of MOs over selected molecular fragments of **M1**

	H-4	**H-3**	**H-2**	**H-1**	**HOMO**	**LUMO**	**L+1**	**L+2**	**L+3**	**L+4**
Energy (eV)	**-6.49**	**-6.47**	**-6.02**	**-5.50**	**-5.11**	**-2.68**	**-1.04**	**-0.98**	**-0.32**	**-0.06**
Alkyl / Aryl	15.00	16.99	13.44	8.14	6.82	19.39	9.24	8.39	**84.17**	**97.40**
BODIPY	0.31	0.26	**68.23**	22.15	**42.62**	**75.55**	18.54	13.28	15.27	2.56
Alkyne	0.30	0.11	4.36	23.90	20.43	2.44	15.49	16.05	0.23	0.00
Thiophene	**84.39**	**82.64**	13.97	**45.81**	**30.12**	2.61	**56.74**	**62.28**	0.33	0.03

Table S2: Computed oscillator strengths (F), positions of the first electronic transitions and major contributions of **M1**

Transition No.	Wavelength (nm)	Osc. Strength	Major contributions
1	594.6	0.8238	HOMO→LUMO (98%)
2	506.3	0.0328	H-1→LUMO (99%)
3	409.0	0.8529	H-2→LUMO (91%)
4	387.9	0	H-5→LUMO (99%)
5	360.6	0.1174	H-6→LUMO (72%), H-3→LUMO (21%)
6	359.2	0.0425	H-6→LUMO (18%), H-3→LUMO (79%)
7	356.7	0.0128	H-4→LUMO (96%)
8	334.1	0.3917	H-7→LUMO (19%), HOMO→L+1 (75%)
9	329.9	0.258	H-7→LUMO (73%), HOMO→L+1 (15%)
10	329.0	0.0492	H-8→LUMO (26%), HOMO→L+2 (64%)
11	320.8	0.0063	H-8→LUMO (69%), HOMO→L+2 (26%)
12	300.9	0.0051	H-1→L+1 (94%)
13	298.6	0	H-9→LUMO (91%)
14	295.7	0.0091	H-10→LUMO (91%)
15	295.2	0.3527	H-1→L+2 (83%)
16	288.3	0	HOMO→L+3 (97%)
17	275.1	0.0333	H-1→L+6 (22%), HOMO→L+5 (63%)
18	272.5	0.0006	H-1→L+5 (30%), HOMO→L+6 (59%)
19	271.5	0.0547	H-2→L+1 (89%)
20	270.2	0.0017	HOMO→L+4 (92%)
21	267.6	0.0012	H-11→LUMO (17%), H-2→L+2 (77%)
22	263.8	0.1438	H-11→LUMO (67%), H-2→L+2 (18%)
23	261.1	0.0003	H-1→L+3 (97%)
24	251.8	0.0627	H-3→L+1 (41%), H-3→L+2 (45%)
25	251.2	0.0989	H-4→L+1 (59%), H-4→L+2 (26%)
26	246.9	0.0001	H-1→L+4 (99%)
27	245.3	0.0013	H-2→L+3 (92%)
28	240.3	0.0002	H-14→LUMO (60%), H-12→LUMO (36%)
29	240.2	0.0007	H-13→LUMO (87%)
30	239.5	0.0156	H-10→L+2 (13%), H-9→L+1 (17%), H-8→L+2 (13%), H-7→L+1 (18%)
31	238.8	0.0219	H-10→L+1 (20%), H-9→L+2 (19%), H-8→L+1 (19%), H-7→L+2 (16%)
32	238.3	0.0004	H-14→LUMO (34%), H-12→LUMO (56%)
33	237.5	0.0001	H-15→LUMO (81%)
34	237.1	0.0053	H-5→L+1 (85%)
35	236.0	0.0203	HOMO→L+8 (24%), HOMO→L+10 (21%)
36	235.6	0.003	H-3→L+1 (41%), H-3→L+2 (33%)

37	235.4	0.0244	H-3→L+2 (11%), H-1→L+10 (10%), HOMO→L+7 (21%), HOMO→L+9 (16%), HOMO→L+11 (12%)
38	234.2	0.0001	H-5→L+2 (84%)
39	233.9	0.0001	H-4→L+1 (32%), H-4→L+2 (65%)
40	233.7	0.0018	H-16→LUMO (81%)
41	233.3	0.0418	H-1→L+5 (36%), HOMO→L+6 (25%)
42	232.5	0.0007	H-18→LUMO (59%)
43	232.3	0.0039	H-1→L+6 (35%), HOMO→L+5 (18%)
44	231.9	0.0039	H-17→LUMO (13%), H-6→L+3 (34%), H-5→L+4 (29%)
45	231.8	0.0006	H-19→LUMO (18%), H-17→LUMO (55%)
46	231.1	0.0228	H-19→LUMO (11%), H-1→L+5 (12%), HOMO→L+7 (17%), HOMO→L+9 (13%)
47	231.0	0.0022	H-6→L+1 (81%)
48	230.3	0.0144	H-19→LUMO (15%), H-2→L+4 (60%)
49	229.8	0.0533	H-19→LUMO (11%), H-2→L+4 (26%), HOMO→L+7 (20%)
50	228.1	0.0006	H-6→L+2 (89%)
51	227.5	0.0047	H-32→LUMO (73%)
52	227.1	0.0163	H-24→LUMO (17%), H-20→LUMO (23%), H-19→LUMO (17%)
53	225.8	0.0455	HOMO→L+8 (30%), HOMO→L+10 (20%)
54	223.8	0.0333	H-21→LUMO (71%), H-20→LUMO (19%)
55	222.3	0.0047	H-24→LUMO (21%), H-23→LUMO (12%), H-20→LUMO (43%)
56	222.2	0.0278	H-10→L+1 (13%), H-9→L+2 (13%), H-8→L+1 (15%), H-7→L+2 (12%), HOMO→L+11 (19%)
57	219.1	0.0011	H-7→L+1 (28%), H-1→L+7 (37%), HOMO→L+8 (15%)
58	218.5	0.0418	H-22→LUMO (72%)
59	217.7	0.099	H-29→LUMO (14%), H-28→LUMO (11%), H-27→LUMO (10%), H-25→LUMO (10%), H-22→LUMO (22%)
60	216.4	0.0458	H-8→L+1 (25%), H-7→L+1 (17%), H-7→L+2 (25%), H-1→L+7 (14%)
61	216.0	0.0981	H-8→L+1 (17%), H-7→L+1 (15%), H-7→L+2 (17%), H-1→L+7 (26%)
62	215.2	0.007	H-25→LUMO (10%), H-24→LUMO (10%), H-23→LUMO (54%)
63	214.8	0.0321	H-8→L+2 (26%), HOMO→L+11 (10%)
64	214.7	0.0096	H-3→L+5 (25%), H-3→L+6 (33%)
65	214.4	0.0526	H-8→L+2 (27%), HOMO→L+9 (13%), HOMO→L+11 (18%)
66	214.1	0.0002	H-4→L+5 (43%), H-4→L+6 (29%)
67	213.9	0.0025	H-26→LUMO (90%)

68	213.5	0.0003	H-27→LUMO (10%), H-25→LUMO (55%), H-24→LUMO (16%), H-23→LUMO (10%)
69	212.7	0.0018	H-40→LUMO (91%)
70	212.7	0.0084	H-2→L+5 (79%), H-1→L+6 (13%)
71	211.4	0.0002	H-3→L+3 (91%)
72	210.9	0	H-39→LUMO (94%)
73	210.8	0.0075	H-2→L+6 (23%), H-1→L+8 (47%)
74	210.5	0.001	H-4→L+3 (89%)
75	210.1	0.0249	H-2→L+6 (56%), H-1→L+8 (17%)

Table S3: Percent distribution of MOs over selected molecular fragments of **M2**

	H-4	**H-3**	**H-2**	**H-1**	**HOMO**	**LUMO**	**L+1**	**L+2**	**L+3**	**L+4**
Energy (eV)	**-6.38**	**-5.95**	**-5.64**	**-5.50**	**-4.90**	**-2.82**	**-1.46**	**-1.42**	**-0.68**	**-0.45**
Alkyl / Aryl	12.12	8.92	8.54	8.23	4.63	13.57	6.43	7.16	9.62	11.63
BODIPY	**83.64**	**85.13**	**48.61**	26.35	**70.37**	**84.12**	**60.51**	**45.03**	**35.70**	**49.17**
Alkyne	0.07	2.42	13.81	22.94	11.17	1.22	9.78	14.07	8.36	5.22
Thiophene	4.17	3.53	29.05	**42.48**	13.83	1.09	23.28	**33.74**	**46.32**	**33.97**

Table S4: Computed oscillator strengths (F), positions of the first electronic transitions and major contributions of **M2**

Transition No.	Wavelength (nm)	Osc. Strength	Major contributors
1	675.6	1.0805	HOMO→LUMO (98%)
2	539.5	0.0366	H-1→LUMO (97%)
3	519.2	0.2584	H-2→LUMO (97%)
4	446.2	0.2949	H-3→LUMO (92%)
5	408.7	0.7023	HOMO→L+1 (91%)
6	405.4	0.4815	HOMO→L+2 (94%)
7	400.0	0.0013	H-9→LUMO (99%)
8	393.5	0.0043	H-4→LUMO (99%)
9	392.9	0.0086	H-5→LUMO (99%)
10	382.3	0.1075	H-10→LUMO (29%), H-8→LUMO (11%), H-7→LUMO (55%)
11	372.2	0.0009	H-6→LUMO (96%)
12	368.9	0.0022	H-8→LUMO (79%), H-7→LUMO (19%)
13	364.2	0.3293	H-10→LUMO (66%), H-7→LUMO (17%)
14	348.6	0.0811	H-11→LUMO (93%)
15	342.0	0.27	H-1→L+1 (78%)
16	335.3	0.0062	H-2→L+1 (15%), H-1→L+2 (49%), HOMO→L+3 (23%)
17	332.5	0.0279	H-12→LUMO (89%)
18	327.5	0.0049	H-2→L+1 (32%), H-1→L+2 (40%), HOMO→L+3 (19%)
19	322.3	0.1589	H-2→L+2 (70%)
20	313.9	0.2015	H-2→L+1 (35%), HOMO→L+3 (43%)
21	310.3	0.0109	H-14→LUMO (72%), H-13→LUMO (15%)
22	307.7	0.0173	H-3→L+1 (34%), H-2→L+2 (11%), HOMO→L+4 (39%)
23	303.0	0.0059	H-15→LUMO (39%), H-14→LUMO (14%), H-13→LUMO (38%)
24	300.9	0.0008	HOMO→L+5 (98%)
25	296.7	0.273	H-3→L+2 (81%)
26	295.7	0.1542	H-3→L+1 (49%), HOMO→L+4 (39%)
27	290.3	0.2081	H-15→LUMO (56%), H-13→LUMO (28%)
28	284.6	0.0055	H-5→L+1 (27%), H-4→L+1 (43%)
29	283.8	0.0062	H-5→L+1 (21%), H-5→L+2 (30%), H-4→L+1 (15%), H-4→L+2 (16%)
30	280.6	0.0058	HOMO→L+6 (87%)
31	279.8	0.0506	H-1→L+3 (60%)
32	276.1	0.0226	H-2→L+3 (25%), H-1→L+4 (17%), HOMO→L+10 (24%)

33	273.4	0.0787	H-2→L+3 (18%), H-1→L+3 (14%), HOMO→L+9 (33%)
34	271.2	0.0548	H-6→L+1 (25%), H-6→L+2 (53%)
35	270.2	0.0446	H-8→L+1 (41%), H-8→L+2 (14%), H-7→L+1 (26%)
36	269.9	0.0234	H-2→L+3 (22%), HOMO→L+9 (15%), HOMO→L+10 (18%)
37	267.1	0.0088	H-8→L+1 (25%), H-7→L+1 (53%)
38	265.7	0	H-5→L+1 (35%), H-5→L+2 (25%), H-4→L+1 (19%), H-4→L+2 (20%)
39	265.2	0.0099	H-4→L+2 (15%), HOMO→L+7 (62%)
40	264.8	0.003	H-5→L+2 (34%), H-4→L+2 (34%), HOMO→L+7 (10%)
41	264.6	0.0043	H-8→L+2 (14%), H-7→L+2 (55%)
42	264.3	0.0207	HOMO→L+8 (78%)
43	261.5	0.0088	H-9→L+1 (87%)
44	261.0	0.0377	H-11→L+2 (16%), H-9→L+2 (21%), H-1→L+4 (10%)
45	260.5	0.003	H-1→L+4 (22%), H-1→L+5 (52%)
46	260.2	0.0017	H-9→L+2 (32%), H-1→L+4 (14%), H-1→L+5 (41%)
47	259.3	0.0081	H-11→L+2 (12%), H-9→L+2 (36%)
48	258.5	0.0076	H-16→LUMO (31%), H-2→L+4 (31%)
49	257.1	0.0029	H-16→LUMO (11%), H-6→L+1 (50%), H-6→L+2 (24%)
50	256.8	0.004	H-16→LUMO (40%), H-6→L+1 (15%), H-2→L+4 (21%)
51	255.6	0.0122	H-14→L+1 (24%), H-14→L+2 (11%), H-12→L+1 (16%), H-10→L+1 (10%)
52	254.7	0.0012	H-2→L+5 (95%)
53	254.5	0.0033	H-8→L+1 (19%), H-8→L+2 (59%), H-7→L+2 (15%)
54	252.5	0.0029	H-10→L+1 (78%)
55	251.5	0.0014	H-10→L+2 (11%), H-3→L+3 (69%), H-2→L+4 (12%)
56	250.6	0.0009	H-11→L+2 (11%), H-10→L+2 (70%)
57	246.3	0.0003	H-19→LUMO (11%), H-18→LUMO (77%)
58	246.2	0.0002	H-19→LUMO (45%), H-18→LUMO (17%), H-17→LUMO (36%)
59	245.6	0	H-1→L+6 (95%)
60	244.3	0.0001	H-19→LUMO (38%), H-17→LUMO (51%)
61	244.1	0.0064	H-20→LUMO (38%), HOMO→L+13 (11%)
62	243.7	0.0156	H-20→LUMO (24%), HOMO→L+12 (16%), HOMO→L+13 (19%)
63	243.3	0.0071	H-3→L+4 (20%), HOMO→L+11 (26%),

			HOMO→L+13 (14%)
64	242.8	0.0284	H-20→LUMO (13%), H-3→L+4 (28%), HOMO→L+12 (11%)
65	242.0	0.0004	H-2→L+9 (16%), H-1→L+10 (18%), HOMO→L+9 (12%)
66	241.7	0.0035	H-2→L+10 (10%), H-1→L+9 (16%)
67	241.5	0.0286	H-25→LUMO (11%), H-23→LUMO (11%), H-21→LUMO (11%), HOMO→L+13 (13%)
68	240.4	0.002	H-11→L+1 (62%), H-11→L+2 (16%)
69	239.7	0.0025	H-2→L+6 (90%)
70	239.5	0.0004	H-21→LUMO (68%)
71	238.9	0.0055	H-5→L+3 (29%), H-5→L+4 (10%), H-4→L+3 (18%)
72	238.9	0.0085	H-5→L+3 (14%), H-4→L+3 (23%), H-4→L+4 (11%)
73	238.2	0.0006	H-24→LUMO (18%), H-12→L+1 (18%), HOMO→L+14 (13%)
74	238.1	0.0001	H-24→LUMO (57%)
75	237.6	0.0005	H-23→LUMO (48%), H-22→LUMO (43%)

Table S5: Lifetime data for **M1** and **9**

	λ_{ex} (nm)		λ_{em} (nm)		$\tau \pm \Delta$ (ns)		χ^2	
	298 K	**77 K**	**298 K**	**77 K**	**298 K**	**77 K**	**298 K**	**77 K**
M1	443	443	650	630	**1.62** ± 0.20 (100 %)	**3.07** ± 0.37 (100 %)	1.051	1.034
9	443	443	650	630	**1.85** ± 0.15 (100 %)	**3.42** ± 0.16 (100 %)	1.051	1.018

SI reference

1. Xia, H. R.; Li, J.; Sun, W. T.; Peng, L. M., Organohalide lead perovskite based photodetectors with much enhanced performance. *Chem Commun* **2014,** *50* (89), 13695-13697.